

# Launch Vehicle Flight Control Augmentation Using Smart Materials and Advanced Composites (CDDF Project 93-05)

---

*C. Barret*  
*Marshall Space Flight Center • MSFC, Alabama*



## TABLE OF CONTENTS

	Page
I. PURPOSE AND INTRODUCTION .....	1
II. MICROELECTRICAL-MECHANICAL SYSTEMS .....	2
III. SMART MATERIALS .....	2
IV. SENSORS .....	5
A. Fully Distributed Sensing of Strain .....	7
B. Strain Sensors With Phase Sensitive Detection .....	8
V. ELECTORRHEOLOGICAL FLUIDS .....	9
VI. PIEZOELECTRICS .....	13
VII. ELECTROSTRICTIVES .....	15
VIII. MAGNETOSTRICTIVES .....	15
IX. SHAPE MEMORY FILMS .....	17
X. SHAPE MEMORY ALLOYS .....	18
XI. ADVANCED COMPOSITES FOR FLIGHT CONTROLS .....	23
XII. CARBON-CARBON COMPOSITES .....	30
XIII. INTERMETALLICS .....	33
XIV. METAL MATRIX COMPOSITES .....	36
XV. TITANIUM MATRIX COMPOSITES .....	41
XVI. CONCLUSIONS .....	47
REFERENCES .....	49



## LIST OF ILLUSTRATIONS

Figure	Title	Page
1.	Impact actuated jump frequency phenomena with MEMS.....	2
2.	Key disciplines of smart flight control technology .....	3
3.	Two approaches to design of smart materials .....	4
4.	Fiber optic smart material architecture .....	7
5.	The ER phenomenon.....	10
6.	ER material behavior .....	11
7.	ER incorporation into the structure .....	11
8.	ER material damping application.....	12
9.	Laminate configuration of different ER fluids.....	12
10.	Embedded PE elements in composite plies.....	13
11.	B-707 aileron test article and deformations achieved .....	17
12.	Superelasticity and shape memory effect.....	18
13.	Martensitic transformation of shape memory alloys.....	19
14.	Using shape memory alloys for variable output actuation .....	19
15.	Shape memory alloy fibers for resonance tuning.....	20
16.	Use of adaptive truss for wing rib .....	21
17.	Active control of wing dynamic response using smart materials .....	21
18.	Smart material helicopter rotor blade.....	22
19.	Tensile stress-strain for Kevlar-49 <sup>TM</sup> .....	23
20.	Composite moduli compared with titanium .....	25
21.	Load deflections for typical 0° unidirectional laminates .....	26
22.	Supersonic missile and fins of polyimide matrix composites.....	27
23.	Construction of Lockheed L-1011 composite aileron.....	28
24.	Typical L/V aerodynamic surface (Saturn IB).....	29
25.	General properties and weaves of carbon-carbon composites .....	31

~~PAGE IV~~ INTENTIONALLY BLANK

PRECEDING PAGE BLANK NOT FILMED

## LIST OF ILLUSTRATIONS (Continued)

Figure	Title	Page
26.	Space shuttle orbiter CCC wing L.E. ....	32
27.	Carbon-carbon strength-to-density ratios.....	32
28.	Carbon-fiber reinforced Airbus fin box .....	33
29.	Melting points of example intermetallics compared to superalloys .....	34
30.	Ti <sub>3</sub> -Al honeycomb structure using diffusion bonding .....	35
31.	Comparison of intermetallics and composites .....	36
32.	Composite groups .....	39
33.	Comparison of metal matrix composite and corresponding intermetallic .....	40
34.	Composite laminae of aerodynamic surface and flight control .....	41
35.	Si-C fiber microstructure .....	42
36.	Tensile exposure result of SCS-9/ $\beta$ 21S composite.....	43
37.	Fiber preforms.....	44
38.	HIP processing of skin panels and stiffeners .....	44
39.	TMC bond strength after testing as depicted by electron micrograph.....	45
40.	Strength comparisons of advanced materials.....	46

## LIST OF TABLES

Table	Title	Page
1.	ER hydrophilics and hydrophobics .....	10
2.	PE material properties .....	13
3.	PE film properties .....	14
4.	Terfenol-D™ material properties .....	16
5.	Comparison of magnetostrictives.....	17
6.	Comparison of smart materials .....	22
7.	Composite flight control applications .....	24
8.	Damping factors of representative laminates.....	25
9.	Coefficients of thermal expansion of representative laminates .....	26
10.	Comparison of composite and metal flight control surfaces.....	29
11.	Composite flight control surface ground tests .....	30
12.	Characteristics of selected intermetallics .....	34
13.	Typical reinforcements used in metal matrix composites.....	37
14.	Mechanical properties of some metal matrix composites .....	38
15.	Desirable characteristics of reinforcing fiber .....	39
16.	Interfacial shear strength of TMC .....	46
17.	Tensile properties of TMC's and other MMC's .....	47





## TECHNICAL PAPER

# LAUNCH VEHICLE FLIGHT CONTROL AUGMENTATION USING SMART MATERIALS AND ADVANCED COMPOSITES

## I. PURPOSE AND INTRODUCTION

The Marshall Space Flight Center (MSFC) has a rich heritage of launch vehicles (L/V's) that have used aerodynamic surfaces for flight stability and control. Recently, due to the aft center-of-gravity (cg) locations on L/V's currently being studied, the need has arisen for the vehicle control augmentation that is provided by these flight controls. Aerodynamic flight control can also reduce engine gimbaling requirements, provide actuator failure protection, enhance crew safety, and increase vehicle reliability and payload capability. In the Saturn era, NASA went to the Moon with 300 ft<sup>2</sup> of aerodynamic surfaces on the Saturn V.

Since those days, the wealth of smart materials and advanced composites that have been developed allow for the design of very light-weight, strong, and innovative L/V flight control surfaces. New areas of engineering design are often born when previously unrelated areas of research evolve to the point where the benefits of their synergistic combination cannot be ignored.<sup>1</sup> Aerodynamic flight control surfaces and smart materials may well be in this class, ripe for technology fusion. A plethora of diverse classes of active materials and advanced composites is available to the flight control design engineer.

Many smart materials can function both as sensors and as actuators. A smart actuator can be a solid, a liquid, or a gas, which changes its character, and hence the character of its surrounding structure. The author has found all of the following terms used in the literature: smart structures, intelligent materials, smart materials, smart composites, smart skins, active structures, active materials, adaptive materials, shape memory effect, shape memory alloys, shape memory alloy hybrid composites, metal matrix composites, and advanced composites, with applications ranging from buildings and bridges to microelectro-mechanical biomedical devices.

The purpose of this paper is to winnow out, from this massive and burgeoning array of smart materials and advanced composites, and assemble in one paper, those that are directly applicable for the flight control surfaces of a L/V. Nowhere in the literature has there been found any applications of smart materials or advanced composites to L/V flight control surfaces.

In this paper, "smart" will denote the ability to sense defined flight parameters, e.g., applied loads, temperatures, or vibration, and actuate an appropriate response in a predetermined and controllable fashion. While smart structures employ sensors, actuators, and control mechanisms integrated into the structure, smart materials can be fabricated in such a manner that sensors, actuators, and control systems will be part of the microstructure of the material itself. Microfabrication technologies, which have evolved from the integrated circuit, are being applied to produce silicon micromechanisms such as integrated sensors and actuators on a chip. Micropumps and valves will deliver microquantities of liquids or gases. As this rapidly growing field of microelectrical-mechanical systems (MEMS) develops, new selections of sensors and actuators will be available for space applications.<sup>2</sup>

## II. MICROELECTRICAL-MECHANICAL SYSTEMS

MEMS have increasing aerospace applications and increase the sampling speed. A valuable data base of microfabrication techniques and actuator designs has emerged. Methods of microactuation include electrostatic and piezoelectric (PE) actuators, fluid expansion, and bimetals. Impact-friction actuated micromechanisms are new actuators in which lateral resonant structures are retracted by electrostatic comb drives and propelled forward toward the actuated micromechanism by elastic forces generated by folded beam flexures at frequencies ranging from 10 to 20 kHz (fig. 1).<sup>2</sup>

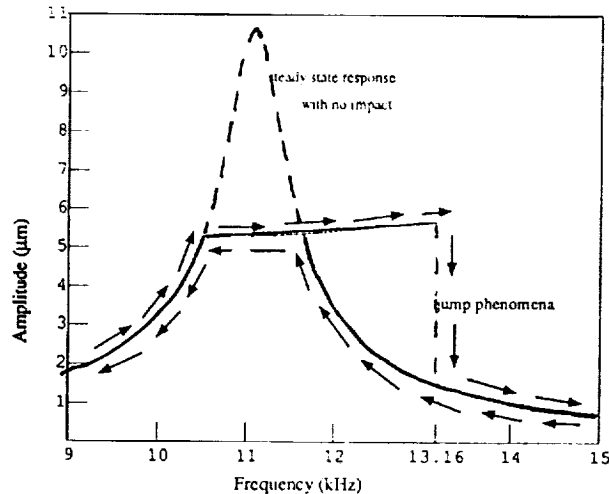


Figure 1. Impact actuated jump frequency phenomena with MEMS.

The jump frequency is a strong function of the coefficient of restitution. Two types of impact actuators are a microoscillator and a polysilicon microvibromotor. Near equiatomic Ti-Ni alloy undergoes a forceful shape recovery due to a crystalline phase change at near ambient temperature. Many active modal modification strategies for vibration control have been demonstrated with a variety of smart materials including Ni-Ti fiber-reinforced epoxy.<sup>1</sup> Shape memory devices are heat actuated. The heat of actuation must be removed before the next cycle can commence. The energy required for miniature actuators can be supplied by small conventional batteries. Ti-Ni actuators change shape about 3 percent. Currently, these devices deliver relatively low forces and small displacements and there are many competing technologies.<sup>2</sup>

## III. SMART MATERIALS

Smart structures and smart materials have emerged during the past few years as 21st century technology. These materials have the inherent ability to interface with modern control systems, and dynamic response characteristics can be actively controlled in real time. They can allow mode suppression, vibration isolation, dynamic alignment, and shape control, and have been successfully demonstrated.<sup>3</sup> Smart flight vehicle skins can determine the presence and amount of ice buildup on critical aerodynamic surfaces. Smart flight controls integrate the technologies of controls, aerodynamics, flight dynamics, sensors, actuators, and materials (fig. 2).

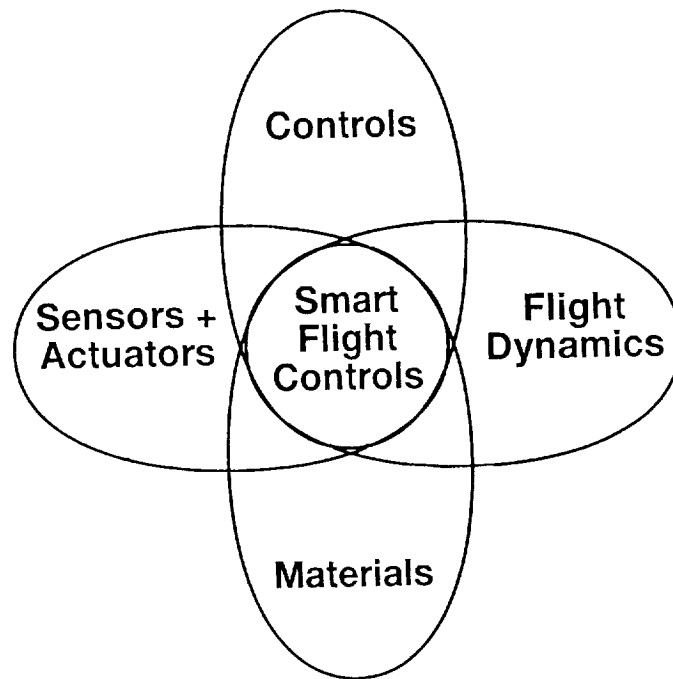


Figure 2. Key disciplines of smart flight control technology.

The dual versatility of some key elements such as piezoelectrics, magnetostrictives, and shape memory alloys can be exploited by employing the same material as a sensor and an actuator. For example, a shape memory alloy could serve as a sensor to monitor ice accumulation or vibration response on a flight control surface prior to becoming an actuator and limiting the amplitude of vibration or ridding the ice. PE ceramics have proven effective both as sensors and actuators in active vibration control and active acoustic absorption.<sup>4</sup> Smart structures have the sensors and actuators embedded into the structure. The ideas are simple. At the structural level, an intimately integrated sensor system provides data on the structure's environment and its loading to a processing and control system which in turn signals intimately integrated actuators to modify the structure's properties in an appropriate fashion. These systems offer immense benefits in space structures applications.

The smart material takes the concept one stage further by an important integration of engineering, material science, chemistry, and physics. The sensing and response functions are built into the material itself using a chemical or morphological structure to provide the responsivity. Photochromics could be classed as smart materials and indeed they are, but the interest is in much more far reaching ideas such as materials which change stiffness, mechanical properties, or even mass under the influence of external fields. These sensing and actuating devices can be easily embedded in advanced composites. A more sophisticated approach is to embed the actuators in the flight controls, also to respond to flight conditions by changing deflection positions. Materials which can physically deform themselves are candidates for smart flight control surfaces. Chemical synthesis methods, such as sol-gel and Langmuir-Blodgett techniques, and physical methods for film formation, such as ion beam deposition and implantation, laser melting and ablation, plasma etching, and chemical vapor depositions have been joined by new classes of techniques which do material manipulation on an atomic scale, such as the scanning tunneling microprobe.<sup>1</sup>

Smart materials are tailored to provide combinations of sensor, information processor, effector, and feedback functions within the materials themselves and to adapt to their environment and provide a useful response to changes. Both the sensor and the actuator functions with the appropriate feedback

must be integrated. There are two main approaches to designing smart materials (fig. 3). One approach combines system sensor, processors and effector functions in a single group. The other approach follows integrated circuit fabrication concepts and uses deposition and materials modification methods to create complex multilayer structures with embedded sensor, memory, logic, and signal functions.<sup>1</sup>

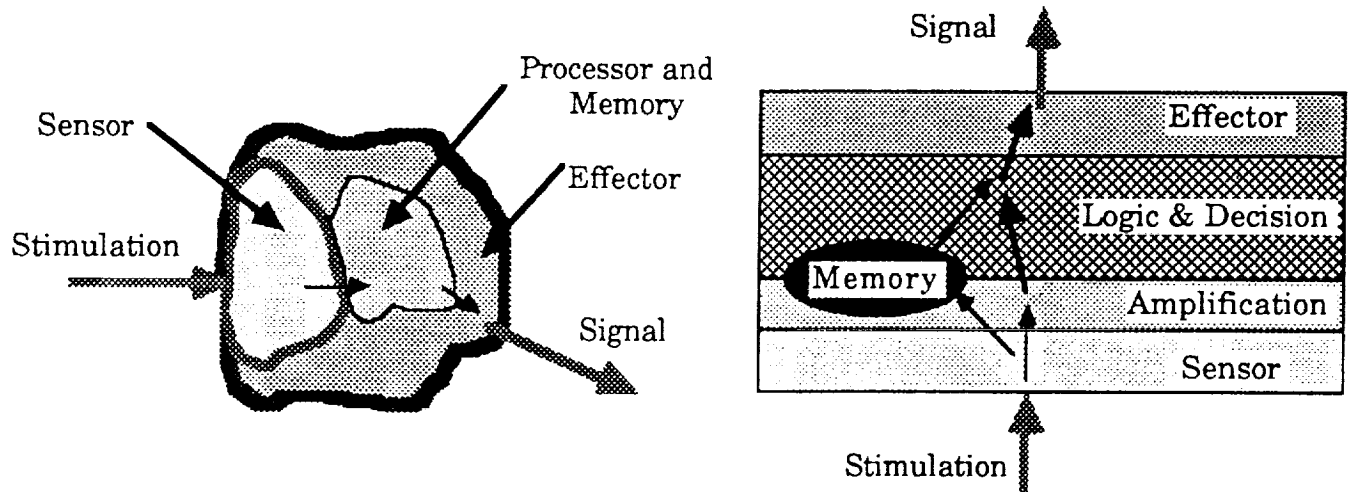


Figure 3. Two approaches to design of smart materials.

In a L/V aerodynamic flight control surface, a basic smart structure could be a surface film on the flight control, which incorporates a network of sensors and acoustic wave generators which could relay flight parameter information such as stress, loading, temperature, dynamic pressure, etc., and respond with flight control actuation. Smart flight control surfaces would require in-flight measurement of rapidly changing dynamic loads on the vehicle. The requirement extends to mechanical vibrations at acoustic frequencies and spatial resolutions of centimeters or better. Active vibration control of smart fibrous composite structures featuring electrorheological (ER) fluids, PE, and fiber optic sensing systems have been demonstrated. Shape memory alloys, PE, and ER fluids have been used to increase aerodynamic efficiency.

Dynamic aeroelastic control uses induced strain actuators such as piezoceramics and electrostrictives which are regulated to apply equivalent forces and moments on the aerodynamic surfaces in order to deform and effect dynamic aeroelastic control. Active surfaces with integrated strain actuators provide a natural mechanism for effecting multiple-actuator dynamic control and for implementing modern model-based control methodologies such as H-infinity. Strain actuated active aerodynamic surfaces can be used for gust and load alleviation (disturbance rejection), flutter and vibration suppression (plant regulation), and maneuver enhancement (command following).<sup>3</sup>

Variable camber has been used to decrease root bending moment, drag, and wind gust response. An F-111 investigation addressed adaptive modifications of wing leading and trailing edges (T.E.'s) to achieve large deformations.<sup>3</sup> It has been shown that significant reduction in shock-induced drag can be achieved by changing shape during flight regime transition. By judicious selection, smart materials can synthesize numerous classes of hybrid actuation systems in order to satisfy a broad range of performance specifications. Some hybrid smart materials feature embedded multifunctional actuation systems that capitalize on the diverse strengths of ER fluids and PE materials and which operate in conjunction with fiber optic sensing systems.<sup>1</sup>

## IV. SENSORS

Optical fiber technology has substantial aerospace and hydrospace usage and provides a basis for gathering data from many points with negligible interference and wide bandwidths. Optical fibers react to temperature and pressure by distorting light. Smart wing leading edges (L.E.'s) with 300 optical sensors in 3 layers have been used by Boeing.<sup>5</sup> McDonnell Douglas has test flown smart structures on the F-15 L.E.'s, and smart helicopter rotors.<sup>5</sup> Fiber optic flight control systems have also been tested in a NASA F-18. Because optical fibers can transmit more than one signal at a time, they offer multiplexing advantages to flight control and can communicate with avionics and actuators. The same fibers that monitor conditions can be used for control. The optimum fibers could be the communication pathway between a L/V's flight controls and its avionics. L/V flight control systems could benefit from fiber optic smart sensors in the manufacturing stage. Fiber sensors embedded in the material could monitor structural changes and vibration, temperature, etc., in support of a vehicle shape control system to allow adaptive guidance. Fiber optic smart structures in combination with actuators have been used for flight vehicle vibration control, localized strain monitoring, and icing control.<sup>1</sup>

A key requirement in a fiber sensor system for smart materials application is compatibility with the composite material. The sensor must not affect the performance of the flight control surface. Glass fibers are very compatible with composite materials. Physical similarities between the optical fibers and the reinforcing fibers used in composites allow the optical sensor to be successfully embedded within the material. Both fibers have similar densities, and optical fibers are capable of withstanding strains of the same magnitude as the composite itself. Although monomode optical fibers can be made as small as 100  $\mu\text{m}$  in diameter, this is ten times the size of a typical reinforcing fiber. For good strain transfer between composite and optical fiber, there must be sufficient bonding. This can be enhanced by the use of suitable coatings. Tensile, compressive, and shear testing of composite materials containing embedded sensors and actuators have indicated minimal effect on the mechanical preparation of the composite. By careful choice of sensors, actuators, their coatings, and host composite compatibility, it is possible to prevent degradation of the mechanical properties of the host composite. It has been shown that embedded arrays of optical fibers had no detrimental influence on the resistance of composites to delamination. It has also been shown that the compressive strength of Kevlar<sup>TM</sup>-epoxy panels is not compromised.<sup>1</sup>

What do embedded optical fibers really measure? Interpretation of signals produced by structurally embedded phase-based optical fiber sensors experiencing thermomechanical loading is complicated because the fiber is subjected to a strain state, which is a tensor quantity, in addition to the scalar temperature field. Therefore, the scalar signal produced by an embedded optical fiber sensor has contributions from a minimum of four quantities; three principal strains and the temperature. Interferometric optical fiber sensors, therefore, do not measure the strain or the temperature directly. They measure the optical phase shifts from which the strain and temperature states are inferred. The interferometric optical fiber sensors are the most prominent in smart materials. Fiber-optic interferometric and polarimetric strain gauges are particularly well suited for embedding into smart composite materials, which could easily be used as flight control surfaces. It has been shown that spatial modulation is applicable to optical fibers braided into a three-dimensional (3-D) composite material, and sensor sensitivity and dynamic range can be improved by special geometrical configurations of the embedded optical fibers (bow-tie and e-core high bi-refrangement fibers), and launching light into one of the eigenmodes of the fiber.<sup>1</sup>

A large body of research has been done on the analysis of intermodal interference patterns to extract information from an optical fiber to determine changing environmental conditions seen by the

fiber along its length. Fiber optic strain gauges compare favorably to the conventional resistive strain gauges. They also allow for additional sensing of the stress fields transverse to the fiber axis. As the applied stress increases, the result is a modal power redistribution caused by intermodal coupling. The modal power redistribution is such that there is a transfer of power to lower-order modes.<sup>1</sup>

Mach-Zehnder, Michelson, and Fabry-Perot are the main dual path interferometric fiber optic sensors used. MBB-Deutsche Aerospace has established teams of researchers to develop smart structures for aerospace applications including automated positioning of flight control systems, flutter suppression, vibration damping, impact detection, and modal analysis of flight controls. Shape control and active vibration damping have been investigated for flight controls in particular. It is hoped that the twist and camber can be optimized for flight conditions. Modal domain interferometric fiber optic sensors are used to detect vibration in smart helicopter blades using embedded PE crystals. Contour holography has also been used.<sup>1</sup>

An autonomous aircraft (A/C) wing and flight control deicing system has been developed by Innovative Dynamics for NASA Lewis Research Center (LeRC). Sensors in the L.E. detect the ice, and then vibrations of the skin are excited to knock it off. The system includes actuator coils, strain sensors, microelectronic circuits, and a microprocessor integrated into modules mounted internally. The module performs two operations: measurement and deicing. During measurement, relatively small excitations are applied to selected coils, and the resulting small vibrations are monitored by the strain sensors. The sensor readings are fed to the central processor, which is programmed to recognize patterns of vibrations that signify various thicknesses and distributions of ice.

When the central processor determines that the ice at a given location is thicker than allowable, the module at that location is commanded to perform the deicing operation in which a much larger excitation is applied to the coils. The resulting larger mechanical impulse knocks the ice off that spot. The system monitors the thickness of ice continually, performing the deicing operation only when and where necessary.<sup>6</sup>

Very high-temperature strain gauges that will operate at temperatures of 2,000 °F and adjust for the thermal components of the output are being developed at LeRC. An active gauge wire is bonded to the strain specimen via a ceramic base coat. An inactive gauge wire made of the same alloy as the active wire is laid out around the active gauge wire. A piece of ceramic cloth is cemented at its edges to the base coat and covers the inactive wire and holds it in loose contact with the base coat. Thus, the strain from the specimen is coupled into the active gauge wire, but not into the inactive wire. The active gauge wires sense the strains, while the inactive gauge wires provide the compensation for the thermal contributions to the gauge readings.<sup>6</sup>

In other flight control embedded sensor applications, the use of composite materials readily allows the embedding of sensors. It may be desirable to measure strain every 10 cm to fully map out the strain field. Two classes of fiber sensors could be used, one set to localize an event and one set to make detailed assessments. The fiber sensors would be very close to the diameter of the fiber, and a number of sensors can be multiplexed along a single fiber line. When existing fiber optic sensors are considered, two candidates for meeting these requirements are fiber optic grating and etalon-based fiber sensors. These sensors may be multiplexed into strings of fiber optic sensors. These strings could be multiplexed using a switch that could be used to interrogate sensors when needed. Figure 4 shows a portion of the fiber optic smart material architecture.<sup>1</sup> A fiber sensor demodulator is used to extract the data from the sensors in the string being accessed. The data are then formatted and transmitted to a system signal processor, which in turn transfers the data to the vehicle assessment system.<sup>1</sup>

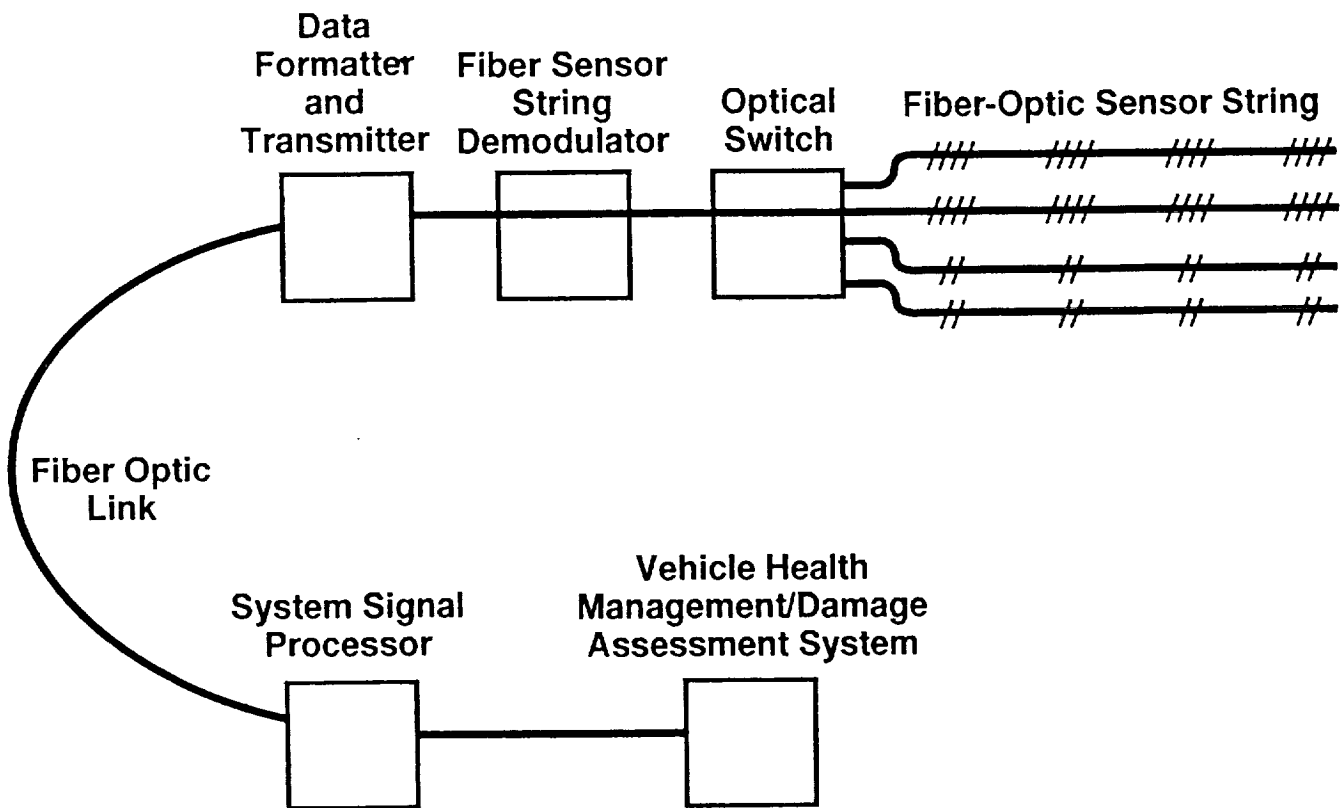


Figure 4. Fiber optic smart material architecture.

### A. Fully Distributed Sensing of Strain

The locations and magnitudes of strain-induced mode coupling and relative changes in propagation constants have been measured using broadband optical sources in two-mode fibers. Differential mode delay occurs between the stress point and the output end of the fiber. This delay can be compensated for at the receiver to permit coherent detection. If a large fraction of the power launched into the sensing fiber can carry the sensor information, performance is improved. System architectures offering efficient use of launched power employ forward scattered light. Two-mode elliptical core fiber sensors have been widely proposed for strain and vibration sensing in smart materials and structures applications. One of the most attractive features of this approach is the single-fiber configuration which can be implemented using insensitive single-mode input and output fibers to interrogate the core sensing section. A two-mode fiber sensor can be viewed as a form of common fiber two-beam interferometric device, where the two beams are formed by the two spatial modes in the fiber. Due to their different propagation constants, there is an effective optical path difference between the modes within the fiber. Remote demodulation of an elliptical-core fiber strain sensor using phase detection developed for two-beam fiber interferometry and multiplexing of core sensors remotely addressed by modulated-source interrogation have been demonstrated by the Naval Research Laboratory.<sup>1</sup>

Proximity sensors are of the transmissive type. They are based on a triangulation technique using optical fibers and graded-index (GRIN) lenses. One fiber provides the illuminating beam, while the other detects parts of the light scattered by the target. Any target displacement in the sensing region gives rise to the intensity modulation of the detected signal. The range of operation and resolution of the sensors can be varied according to the geometrical arrangement of the optical head. These sensors can operate as

on/off switches as well as analog sensors. A differential two-core fiber can be used for separate measurement of strain and temperature, and a dual-wavelength technique can be used to perform absolute measurements over an extended dynamic range for aerospace applications. Interferometry has the advantage of high sensitivity with low power levels. To be able to measure strain over a wide temperature range, the system must monitor both temperature and strain simultaneously, and two-core fibers are suited. The cores should work as independent waveguides.<sup>1</sup>

### **B. Strain Sensors With Phase Sensitive Detection**

Bragg grating sensors are useful for quasi-static distributed sensing in smart structures and materials for the real time evaluation of load, strain, temperature, vibration, etc. Their wavelength-encoded nature of output has distinct advantages over direct intensity based sensing schemes. As the sensed information is encoded directly into the wavelengths, which is an absolute parameter, the output does not depend on the total light levels, losses in the connecting fibers and couplers, or source power. The means to detect wavelength shifts of a grating sensor are based on the use of an unbalanced fiber interferometer wavelength discriminator. The wavelength component, reflected back from a fiber grating illuminated by a broadband source, is fed to an unbalanced Mach-Zehnder interferometer. This light becomes the source into the interferometer, and wavelength shifts induced by perturbation of the grating resemble a wavelength modulated source.<sup>1</sup>

This concept has been widely used in the field of interferometric fiber sensors to introduce a phase carrier signal into an unbalanced interferometer using direct laser emission-frequency modulation for the purpose of phase demodulation. The converse of this can also be used. The unbalanced interferometer can be used as a discriminator to detect the wavelength shifts in the effective source formed by the strained grating element. High resolution techniques for detection of dynamic strain-induced shifts in the reflection wavelength of an in-fiber Bragg grating sensor have been demonstrated. Dynamic strain resolution at frequencies above 100 Hz has been demonstrated by the office of Naval Research.<sup>1</sup>

Fiber optic grating sensors are produced by exposing an ultraviolet (UV) beam on a short length of an optical fiber by a transverse holographic method. The UV beam causes permanent changes in the index of refraction along a small part of the fiber. If broadband light is sent into the fiber, there will be notches and peaks in the transmitted and reflected spectrum, respectively, where the Bragg condition is satisfied. By using fiber optic gratings with different wavelength, one optical fiber can be used for spatially distributed sensing.<sup>1</sup>

Optical fibers, transducers, and PE skins have been used for structural vibration and shape control. The upper operational temperature of silica-based optical fiber sensors is about 1,000 °C; other optical sensors, e.g., sapphire based, have demonstrated use at 2,000 °C. In addition to optical sensors, PE film can be sputtered onto a metal fiber. This active sensor develops an electric field when strained and can detect vibration as well as fracture in a manner similar to acoustic emission. These are well suited for embedding in composite materials and have been successfully tested in carbon composite beams and filament wound cylinders at vibration frequencies of 2,100 Hz.<sup>1</sup> Flight vehicle smart skins incorporate PE film modal sensors which supply information on individual dynamic mode shapes. A direct measurement of the natural modes of vibration could help eliminate the control system estimation techniques based on complex algorithms that decompose a vibration into natural modes. In-flight A/C deicing systems using PE films to sense change in wing vibration signature that result from ice buildup could be used for L/V flight control surfaces.



Two new sensor-related technologies, silicon micromachined sensors and polyimide-based waveguide structures, have been developed (Honeywell) that make acoustic waveguide sensors available for smart flight control surfaces. In the silicon micromachined sensors, applied pressure exerts a force that deflects a diaphragm which delivers an applied stress to the micromachined sensor area. The sensor chip features an active partitioned sensor region; typical sizes are 10 to 100  $\mu\text{m}$ . Polyimide-based waveguide structures are optical waveguides or light pipes featuring micrometer-level sizes and surface conformal construction relevant to smart materials applications. Key benefits of the polyimide optical waveguide structures for smart surface applications include high-bandwidth throughput ( $> 10$  GHz) and electromagnetic interference immunity. They could be easily embedded into composite smart flight control surfaces or conformally applied to metallic flight control surfaces. Honeywell investigations indicate that propagation losses of 0.01 dB/cm are soon achievable. Optical waveguide sensors featuring a silicon chip assembly have been designed for flight vehicle smart material applications. Incident light is coupled onto the sensor assembly from the optical fiber connected to the flight vehicle support avionics interface. Optical power is sourced from an avionics interface. Individual sensors are interconnected by an optical bus medium as a fault-tolerant communications network. The incoming light is coupled onto the sensor via a GRIN lens to minimize optical alignment problems due to temperature coefficient differences between the sensor assembly and the smart material. Mechanical vibration causes the sensor's cantilever beam to oscillate, which interrupts the passage of light through the waveguide assembly. The optical light is either intensity-modulated or wavelength-modulated, depending on the application, and coupled back to the flight vehicle avionics interface for detailed analysis. These sensors have low-profile conformal packaging and high-temperature operation ranges.<sup>1</sup>

Optical fiber sensors for A/C damage monitoring can detect cracks of 5 to 30  $\mu\text{m}$  in Al alloys. Fabry-Perot sensing systems have been designed for aerodynamic surface shape control and vibration damping. To detect force, pressure, and bending, PE is the best fiber-optic sensor.<sup>4</sup> Sensors embedded in the L/V flight control surfaces could record load histories. Embedded pressure sensors would be the ideal.<sup>7</sup> Embedded fiber optic-based sensors have demonstrated the ability to detect impact damage on flight control surfaces for the purpose of in-flight reconfiguration of the flight controls. The sensor output can be interpreted and passed to the vehicle control system for actuation of embedded actuators, and smart flight control surfaces could measure their own loads. Whereas PE and strain gauges give local domain information, the fiber optic interferometer and shape memory alloy methods give integrated global information.<sup>1</sup>

## V. ELECTORRHEOLOGICAL FLUIDS

ER fluids are one class of smart materials that change rheological characteristics very rapidly when electric fields are applied and can provide rapid response in controlled mechanical devices. This change in behavior in the presence of an electric field renders them suitable to control variable stiffness or damping in a material. The ER fluids are typically suspensions of micron-sized hydrophilic particles suspended in suitable hydrophobic carrier liquids, that are Newtonian (free-flowing) with no field present, but stiffen reversibly to a non-Newtonian fluid, or a solid as field strength increases so that viscosities are adjustable (fig. 5 and table 1).<sup>4</sup> When these fluids are embedded in voids in structural materials, the imposition of an electric field permits the mechanical properties of the material to be actively controlled. The voltages required to activate the phase change are typically 1 to 4 kV/mm of fluid thickness, but since current densities are in the order of 10 mA/cm<sup>2</sup>, the total power required to change properties is quite low.<sup>4</sup> Both hydrous and anhydrous ER fluids have been studied. Hydrous systems were restricted to small ranges of operating temperature, but the new generation of anhydrous ER fluids have overcome this limitation.<sup>1</sup>

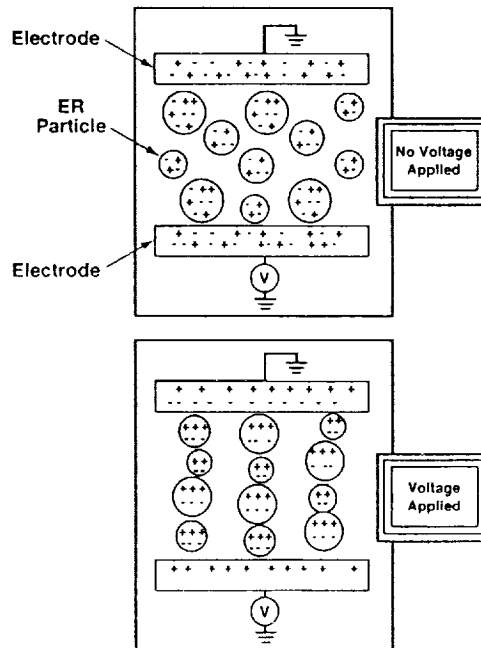


Figure 5. The ER phenomenon.

Table 1. ER hydrophilics and hydrophobics.

Solute	Solvent	Additive
Kerosene	Silica	Water and detergents
Silicone oils	Sodium carboxymethyl cellulose	Water
Olive oil	Gelatine	None
Mineral oil	Aluminum dihydrogen	Water
Transformer oil	Carbon	Water
Dibutyl sebacate	Iron oxide	Water and surfactant
Mineral oil	Lime	None
P-xylene	Piezoceramic	Water and glycerol oleates
Silicone oil	Copper phthalocyanine	None
Transformer oil	Starch	None
Polychlorinated biphenyls	Sulphopropyl dextran	Water and sorbitan
Hydrocarbon oil	Zeolite	None

ER materials, noted for very fast response times, have many aerospace applications as both sensor and actuator where stiffness, damping, and natural frequencies of flight control surfaces can be dramatically changed in milliseconds and where variable performance is required.<sup>1</sup> Using Bingham plastic ER material behavior and steady-state condition, the relationship between flow rate and pressure drop for a configuration can be determined.<sup>8</sup> ER adaptive structures are primarily based on the controllability of the pre-yield rheology of ER suspensions. Two basic configurations of ER materials that have been incorporated in the structure and studied include the shear and the extensional configurations (figs. 6<sup>1</sup> and 7).<sup>1 8</sup> Controllable devices are mostly based on post-yield shear behavior of ER suspensions. Adaptive structures are made controllable through the incorporation of ER materials at selected locations. Controllable valves were some of the first ER devices investigated. They contain fixed electrode configurations with an ER suspension material flowing through. The pressure drop across and

flow rate through the device is controlled by an electric field. Benefits of ER valves include fast response time and freedom from mechanical moving parts. Valve pressure drops as high as 1,000 lb/in<sup>2</sup> have been achieved, and modulation frequencies on the order of several hundred hertz have been realized. Studies of ER shakers have demonstrated that high force output and wide operational bandwidth are possible. ER controllable machinery and engine mounts have been widely investigated

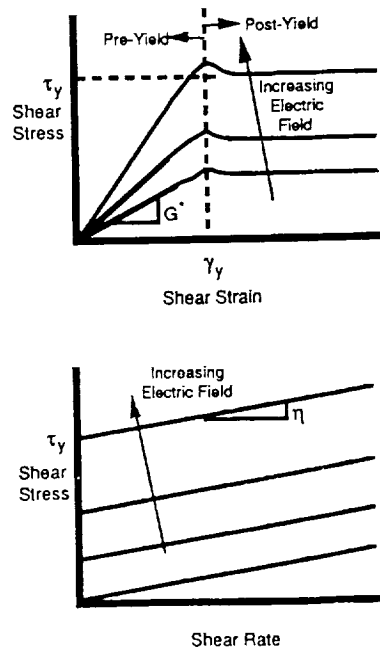


Figure 6. ER material behavior.

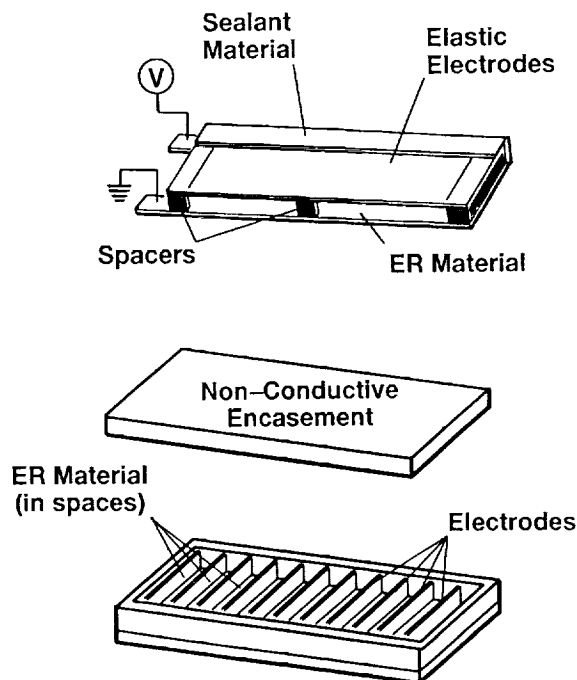


Figure 7. ER incorporation into the structure.

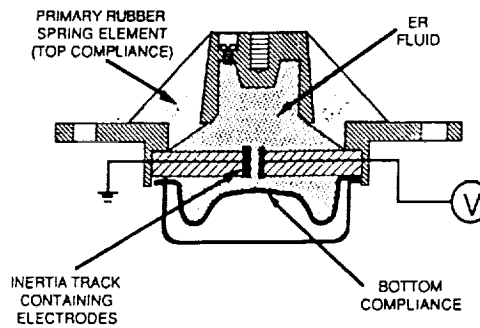


Figure 8. ER material damping application.

(fig. 8).<sup>8</sup> Controllable mounts in the 1 to 50 Hz range having two states, a low damping off-state and a very high damping on-state, have demonstrated long duration testing and positive control at temperatures of 110 °C. Response times of less than one millisecond, sinusoidal force patterns with amplitudes of 2,200 lb, and frequencies of 1,000 Hz have been demonstrated by ER shakers.

ER dampers have been investigated for A/C landing gear components and large damping struts to reduce vibrations. ER materials have been applied to A/C wings and helicopter rotors to control stiffness of each blade independently and are suited to flight control surfaces. These systems sense external stimuli and react in an appropriate manner so as to meet prespecified performance criteria.<sup>1</sup> They can modify the natural frequency of a system by sensing the dominant vibration frequency band and adjusting its viscosity.<sup>7</sup> The helicopter dampers handle dynamic loads of 2,000 N over a frequency range of 0 to 20 Hz. Struts have been laboratory tested up to frequencies of 150 Hz.<sup>8</sup>

Smart composites featuring ER fluids have been investigated for flight vehicle applications at Michigan State University. Dynamically tunable ER fluids contained in voids of the composite can be used for flight control surface vibration control.<sup>8</sup> Magnetorheological fluids have also been used for vibration control.<sup>3</sup> Some A/C programs are nonarticulating flight control surfaces, where the appropriate regions at the edges of the relevant airfoil sections deform in order to provide the aerodynamic control required. Many programs are in progress for smart wings to control dynamic response.

Active dampers utilizing ER fluids have been used for missile flight control fin actuation systems. The program features fins that can be electrically switched between conductive and nonconductive states for microwave shielding application. Laminates can utilize different ER fluids to design specific properties (fig. 9).<sup>4</sup>

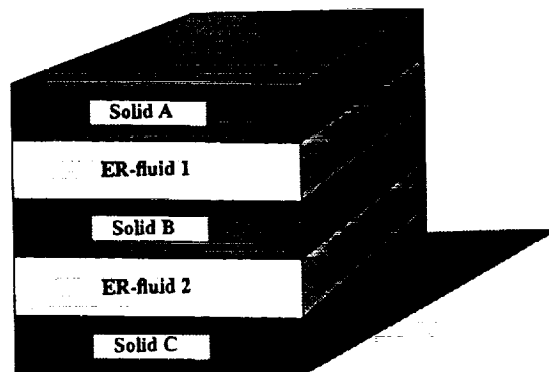


Figure 9. Laminate configuration of different ER fluids.

## VI. PIEZOELECTRICS

PE materials are solids capable of exerting mechanical forces in response to an applied voltage, or vice-versa; consequently they can be used as either sensors or actuators in smart materials. PE actuators permit controlled voltages to generate axial forces or bending moments. Lead zirconate titanate,  $\text{Pb}(\text{Zr,Ti})\text{O}_3$ , commonly referred to as PZT, exhibits a strong PE effect. The deformation is linear with respect to the applied field and changes sign when the electric field is reversed. PZT actuators have been used in active mirror control for many years. Tables 2<sup>4</sup> and 3<sup>7</sup> show typical properties. Their faults are hysteresis and aging. The Curie temperature of a PE material defines its thermal limit, some as low as 200 °F. The current generation of smart PE materials is synthesized with composite laminates (fig. 10).<sup>4</sup>

Table 2. PE material properties.

Property	Units	PVDF	PZT	Bz-Ti-O <sub>3</sub>
Density	(10 <sup>3</sup> ) kg/m <sup>3</sup>	1.78	7.5	5.7
Relative permittivity	$\epsilon/\epsilon_0$	12	1,200	1,700
$d_{31}$ Constant	(10 <sup>-12</sup> ) m/V	23	110	78
$g_{31}$ Constant	(10 <sup>-3</sup> ) V m/N	216	10	5
$k_{31}$ Constant	percent at 1 kHz	12	30	21

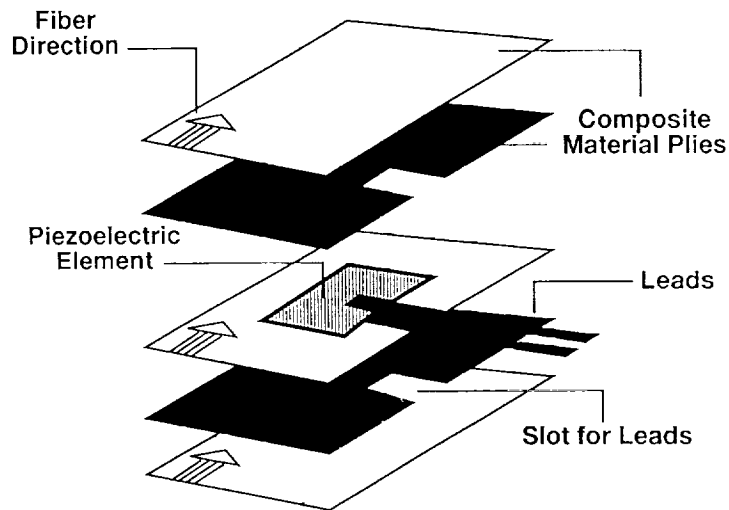


Figure 10. Embedded PE elements in composite plies.

PE materials have been used for vibration control on helicopters, and aeroelastic applications have been investigated to reduce fatigue and flutter induced by aerodynamic buffeting in flight control surfaces, fins, canards, and wings, by NASA LaRC. Aeroelastic control of A/C wings using embedded PE materials in proportion to the wing root loads has been demonstrated by McDonnell Douglas. Flexural axis position has been controlled by the feedback gain which has controlled the lift effectiveness. Placing the flexural axis ahead of the wing aerodynamic center can cause elastic wing lift to be greater than the lift of a rigid wing of the same geometry. This effect can be used to reduce the effect of gust loads. Variable feedback gain also controls the effective bending and torsion.<sup>3</sup>

Table 3. PE film properties.

Property	Value
Thickness	9,28,52,110 $\times 10^{-6}$ m
Piezoelectric strain constant - $d_{31}$	23 $\times 10^{-12}$ $\frac{\text{m/m}}{\text{V/m}}$
Piezoelectric strain constant - $d_{33}$	-33 $\times 10^{-6}$ $\frac{\text{m/m}}{\text{V/m}}$
Piezoelectric stress constant - $g_{31}$	216 $\times 10^{-3}$ $\frac{\text{V/m}}{\text{N/m}^2}$
Piezoelectric stress constant - $g_{33}$	-339 $\times 10^{-3}$ $\frac{\text{V/m}}{\text{N/m}^2}$
Electromechanical coupling factor	12 percent (at 1 kHz) 19 percent (at 1 kHz)
Capacitance	380 pF/cm <sup>2</sup> for 28 $\times 10^{-6}$ meter film
Young's modulus	2 $\times 10^9$ n/m <sup>2</sup>
Speed of sound	1.5 to 2.2 $\times 10^{-3}$ m/s (transverse thickness)
Pyroelectric coefficient	-25 $\times 10^{-6}$ C/m <sup>2</sup> K
Permittivity	106 to 113 $\times 10^{-12}$ F/m
Relative permittivity	12-13
Mass density	1.78 $\times 10^3$ kg/m <sup>3</sup>
Volume resistivity	10 <sup>13</sup> ohm meters
Surface metallization	2.0 ohms/square for Cu-Ni
Resistivity	0.1 ohms/square for Ag ink
Loss tangent	0.015 to 0.02 (at 10 to 10 <sup>4</sup> Hz)
Compressive strength	60 $\times 10^6$ N/m <sup>2</sup> (stretch axis)
Tensile strength	160 to 300 $\times 10^6$ N/m <sup>2</sup> (Transverse axis)
Temperature range	-40 to 80 °C
Water absorption	< 0.02 percent H <sub>2</sub> O
Maximum operating voltage	750 V/mil = 30 V/10 <sup>-6</sup> m
Breakdown voltage	2,000 V/mil = 100V/10 <sup>-6</sup> m

By incorporating PE rods into a composite material, directional actuation can be achieved, and applications include shape control of a wing or a deflection of a control surface, although shape memory alloys would allow larger deflections. The undesirable aging fault would not affect use on an expendable L/V. Hysteresis and temperature limits, however, would have to be considered. These are nonlinear at high applied voltage levels and larger deformations.<sup>7</sup> Beam tip deflections and axial extensions have been demonstrated with piezoelectrics.<sup>4</sup>

Active aeroservoelastic missile fins using directionally attached piezoelectric (DAP) actuator elements have been developed. This fin uses a NACA 0012 airfoil and has been wind tunnel tested to within 6 percent of predicted static deflection.<sup>3</sup> Smart surfaces can be used for gust load reductions and

L/V trim. Using adaptive controlled surfaces with smart materials for actuators, aeroelastic interaction can be tailored to produce new forces and control torques.

Most actuator systems are pneumatic, hydraulic, or electromechanical and occupy from 2 to 6 percent of fuselage volume. Because these actuators are mounted within the fuselage, they cannot be placed adjacent to flight control surfaces and require bearings and linkages. A fin actuator contained entirely within the aerodynamic surface will occupy no fuselage internal volume. A smart torque plate integrated into a fin could generate pitch deflections of the fin as a solid-state flight control actuator. Solid-state flight control surfaces using smart materials have been investigated. It has been shown that extremely small amounts of smart deflection could be effectively magnified by the dynamic pressure of the air flow. Performance of low aspect ratio wings have been studied using active camber and twist control. From studies of polyvinylidene film, PE fiber composites, and conventionally attached and DAP element actuator materials, it has been shown that torsional actuation favors highly orthotropic actuation elements. Of the materials studied, DAP elements generated deflections and moments that were double that of other materials. An active torque plate has been integrated into a 66- by 93-mm missile fin to produce pitch deflections in excess of  $\pm 3^\circ$  and grow with increasing airspeed.<sup>3</sup>

## VII. ELECTROSTRICTIVES

Because of the high hysteresis of PE materials, electrostrictives were developed. In electrostriction, the strain is linearly proportional to the square of the applied electric field. A PE crystal generates strain. The operating principle involves the diffuse phase transition of a relaxer ferroelectric material upon the application of an electric field. The electrostrictive phenomenon is attributed to the rotation of small electrical domains when an external electrical field is imposed. In the absence of this field, the domains are randomly oriented. The alignment of these electrical domains parallel to the electrical field results in the development of a deformation field in the electrostrictive material.<sup>4</sup>

The electrostrictive ceramic compound lead-magnesium-niobate (PMN) exhibits shape memory effects with an electric field. The thermoelectrostrictive effect and the quadratic electrostrictive phenomenon are dependent upon the temperature. This type of material, while exhibiting less hysteresis than piezoceramics, features a nonlinear constitutive relationship requiring some biasing in practice to achieve a nominally linear relationship over a limited range of excitation.<sup>4</sup>

## VIII. MAGNETOSTRICTIVES

These solid materials act similarly to the PE materials, only they respond to magnetic rather than electric fields and are the magnetic analog of electrostrictives. The magnetostriction phenomenon is attributed to the rotations of small magnetic domains in the material, which are randomly oriented when the material is not exposed to a magnetic field. The orienting of these small domains by the imposition of a magnetic field results in the development of a strain field. As the intensity of the magnetic field is increased, more magnetic domains orientate themselves so that their principle axes of anisotropy are colinear with the magnet field in each region and finally saturation is achieved. Terbium-iron alloys are typical magnetostrictive materials.<sup>4</sup>

These materials have large energy density and high modal damping, and they convert strain energy into a magnetic field which produces voltage and current in a transducer coil. High force, high

strain, wide bandwidth, and linear actuators are available, driven by the new class of giant magnetostrictive materials such as Terfenol-D™. Terfenol-D™ is for terbium (Ter), iron (Fe), dysprosium (D) and Naval Ordnance Laboratory (NOL) and uses the form  $Tb_xDy_{1-x}Fe_2$ , a common example of which is  $Tb_{0.3}Dy_{0.7}Fe_2$ .<sup>9</sup> A solenoid is used to supply the magnetic field and a Terfenol™ rod is used to supply the strain. The Terfenol™ core is placed inside a solenoid, and a current is passed through the solenoid inducing a strain in a direction along the core axis. The Terfenol™ rod is then elongated. The displacement is proportional to the magnetic field intensity. The Terfenol-D™ drive element is sized based on the force and displacement requirements. Terfenol-D™ actuators are known for high energy density, thus a compact actuator can produce a high force. Terfenol™ actuators offer improvements over stacked PZT devices with no aging effects or thermoelastic creep and operate in temperatures over 300 °C.

Studies using Terfenol-D™ in dampers, actuators, and velocity sensors have been done by Satcon Technology Corp. for MSFC. It has been shown that Terfenol-D™ has a wide temperature operating range from above room temperature to cryogenic, and that it is a competitive alternative to PE actuators (table 4). Strokes over 100  $\mu m$  and forces of 1,700 N are available from small actuators. The self-sensing capabilities of Terfenol-D™ actuators allow development of smart actuators.

Table 4. Terfenol-D™ material properties.

Property	Value	Units
Density	$9.25 \times 10^3$	kg/m <sup>3</sup>
Young's modulus	$2.5 \text{ to } 3.5 \times 10^{10}$	N/m <sup>2</sup>
Tensile strength	28	MPa
Compressive Strength	700	MPa
Thermal expansion	$12 \times 10^{-6}$	°C <sup>-1</sup>
Resistivity	60	$\mu L \text{ cm}$
Relative permeability	5 to 10	
Coupling factor	0.7 to 0.75	
Sound speed	1,720	m/s
Magnetostriction	1,520 to 2,000	p/m
Energy density	$1.4 \text{ to } 2.5 \times 10^4$	J/m <sup>3</sup>

Magnetostrictives have been used for flight control surface vibration and flutter suppression and for airfoil camber optimizations (Naval Surface Weapons Center). To control stutter in canard, fins, and wings, the critical vibration modes must be damped. A L/V goes through three speed regimes during its ascent trajectory and may be subject to undesirable flight control surface vibrations. A NASA LaRC study has shown Terfenol-D™ to have superior strength, higher modulus, and wider operational bandwidth than shape memory alloys. It can generate enough force to overcome the aerodynamic loads on a flight vehicle and has a low magnetic field requirement. Magnetostriction devices are currently being evaluated for shape change of control surfaces on torpedoes and gimbaling of flight deck simulators. Also being evaluated is an integrated actuation system for individual control of helicopter main rotor blades using Terfenol-D™ actuators to provide higher harmonic control of the individual blades.<sup>7</sup>

Aerodynamic surface applications of twist control as well as camber control have demonstrated that significant deflections can be produced. Air loads can be used to further twist a flight control surface. Aileron deflections of 31°/m in twist, and 44°/m in bending have been demonstrated.<sup>1</sup> Grumman Aircraft is using Terfenol-D™ for the control of A/C flight control surfaces. They have



shown that a Boeing 707 A/C wing can be adaptively deformed over its entire cross section to use optimized aerodynamic shape for varying flight speed regimes. Terfenol-D™ actuators meet the load requirements while being light in weight. Ribs and spars are replaced with smart members containing rods of Terfenol-D™. In order to maximize the displacement obtainable, a diamond-shaped structure was constructed which deflects the T.E. by 60° (fig.11).<sup>7 1</sup> This technology has great potential in the area of aeroservoelasticity. Higher power versions of Terfenol-D™ smart materials are being developed by Etrema Products, Inc., under a \$250,000 Navy contract. Table 5 shows magnetostrictive material comparisons.<sup>7</sup> While Terfenol-D™ has 35 times larger strains than Metglas, it cannot yet be laid into composites.<sup>7</sup>

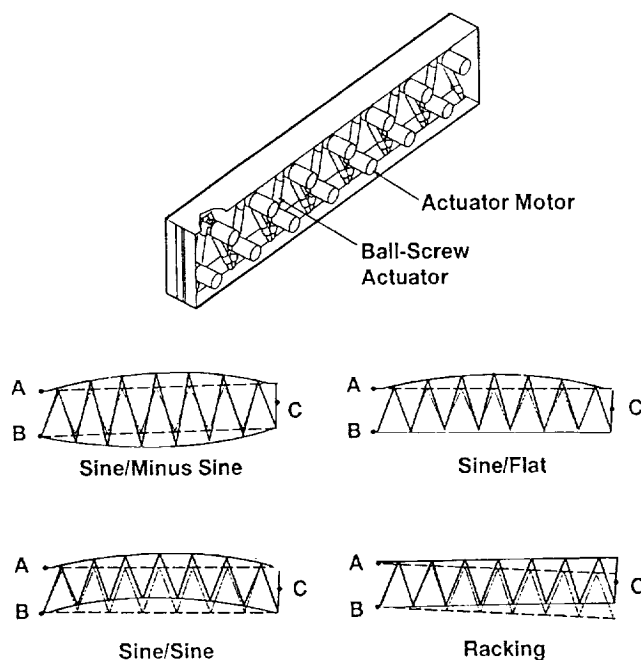


Figure 11. B-707 aileron test article and deformations achieved.

Table 5. Comparison of magnetostrictives.

	Nickel	Metglas	Terfenol-D™
Maximum Strain	50 p/m	50 p/m	1,800 p/m
Field Required	6,000 G	1 G	500 G
Resistivity	$7 \times 10^{-8} \Omega\text{m}$	$1 \times 10^{-6} \Omega\text{m}$	$6 \times 10^{-7} \Omega\text{m}$
Available in foil	yes	yes	no

## IX. SHAPE MEMORY FILMS

Shape memory ferroelastic and ferroelectric thin films have dramatically dependent mechanical properties as their key feature. These are associated with a first-order martensitic transformation from a high-symmetry high-temperature austenitic phase and a low-symmetry low-temperature martensitic phase. The low-temperature phase is easily twinned into many crystallographic twin variants, with one crystallographic twin growing at the expense of the others with an applied stress. On heating, the twins revert to their original configuration before transformation into the austenitic phase.

Macroscopically, the martensitic material is easily deformed through the growth of these twins, which can accommodate plastic true strains which are recovered on heating, through transformation into the high-temperature phase and shape, hence the term shape and memory effect (SME). Ti-Ni for example, changes 12 percent in resistance with an increase in stress, which makes it a useful sensor material (fig.12). When the material is in its high-temperature phase, large stresses cause isothermal transformation back to the lower-symmetry phase, which can be deformed several percent. On release of the stress, the material reverts back to the austenitic phase with complete recovery of the deformation. The isothermal nature of the deformation has been termed superplastic. Alloys which exhibit SME include: Au-Cd, Ag-Cd, In-Tl, Cu-Al-Zn, Cu-Al-Ni, Ti-Pt, Ti-Nb, and Ti-Ni.<sup>2</sup>

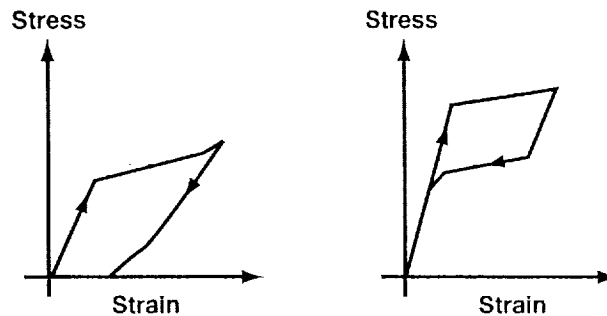


Figure 12. Superelasticity and shape memory effect.

The SME is not limited to metals. Shape-memory-plastics, such as Norsoex and Zeon Shable, have also been developed. Mechanical work has also been obtained from the 15-percent expansion of paraffin. High-output paraffin positioning actuators have been used to produce 150 lb forces over 0.1 in displacements when powered by 20 W at 28 V. This method can be used to address dynamic response versus load for accurate positioning for <1 Hz. Shaft extensions result from pressures of 10,000 lb/in<sup>2</sup>. Actuation temperatures are 60 to 110 °C. On cooling, the paraffin begins to solidify after 1.5 °C of thermal hysteresis. Then the actuators retract.<sup>4</sup>

## X. SHAPE MEMORY ALLOYS

Shape memory alloys (SMA's) are a special class of smart materials which convert thermal energy into mechanical work and are ferrous and nonferrous. There are more than 10 basic SMA's. Some of the most common materials are Nitinol™ (12,000 lb/in<sup>2</sup> yield strength and 6-percent strain limit), a titanium and nickel alloy named for the Naval Ordnance Laboratory (see above), Cu-Zn-Al, Cu-Al-Ni, and Fe-Mn-Si. SMA's change shape as a function of temperature due to a crystalline phase change. This process occurs between the two different crystalline phases of the alloy, austenite and martensite. Martensite is the low-temperature phase, while austenite is the high-temperature phase that forms above the critical transition phase. The change in crystal structure is from an ordered cubic crystal to a monoclinic crystal phase upon the application of heat. The monoclinic phase has no equal sides and no right angles. To undergo the martensitic transformation, first observed by the German metallurgist, Adolf Martens, the material forms alternate bands or twins, an extremely fine structure of the characteristic martensitic microstructure (fig. 13).<sup>4</sup> In the soft martensitic state, little force is required to align the twins and deform the material. Upon application of heat, the phase change to the face-centered cubic austenitic state restores the shape and generates significant force and deformation in the process. As shown by studies done for MSFC by E\*Sorb (1992), SMA's can be used to do impressive physical work.

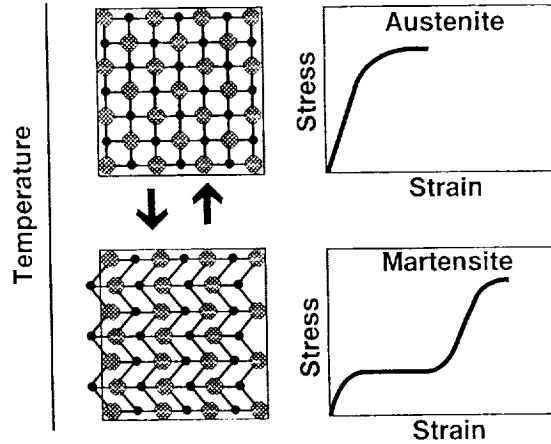


Figure 13. Martensitic transformation of shape memory alloys.

The fundamental characteristic of the reversible SMA is that regardless of the severity of the deformation of the low-temperature martensitic phase, heating induces a reverse transformation which allows return to the original shape at the high-temperature austenitic phase. The heat can be produced by fluids or electricity. If the heating and cooling is controlled by pulsed direct electric current, repeated cyclic motions with high degrees of accuracy can be achieved.<sup>7</sup> The entire subject of martensitic phase transformations is one of considerable technological interest. Understanding the basic physical phenomena has been aided by applying finite element techniques to solve continuum elastic models for phase transitions and by considering atomistic model Hamiltonians of a martensitic system.<sup>4</sup>

SMA's have been utilized both as actuators and as sensors. The Ni-Ti family exhibit good force output and comparatively low hysteresis. SMA actuators are typically actuated by electric current. The transformation temperature of these materials can be selectively tuned over a broad range, and temperature hysteresis has been improved to <2 percent. The Intelligent Materials Laboratory at Michigan State University has developed a new class of SMA actuators which deliver variable output (fig. 14).<sup>4</sup> The response time of the SMA actuator is directly controlled by the cooling rate. In an expendable L/V, the cryogenics may be used to assist with the cooling rate, and the number of load cycles would not be a limiting factor for the application considered in this paper.

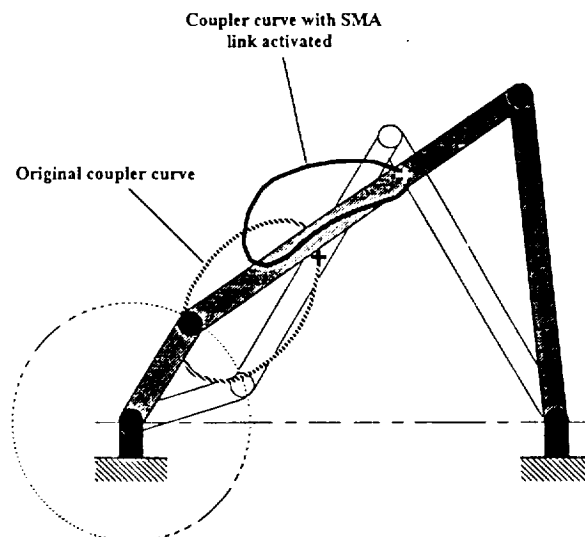


Figure 14. Using shape memory alloys for variable output actuation.

SMA devices have already proven their importance in dynamic systems by controlling vibrations in flexible beams. SMA unique characteristics include their Young's modulus of elasticity (E), temperature relations, damping characteristics, and tunable E and recovery force. Tuning the properties or recovery stress requires heating or cooling, which may not be suitable for high-frequency vibration control but good for low-frequency control. The high damping capacity of the martensitic phase of SMA's can be used in passive vibration control. The hysteretic damping of pseudoelastic SMA's can be exploited in passive/adaptive vibration control. The E of high-temperature austenite is three to four times as large as that of low-temperature martensite. Shear modulus has the same relation. When Nitinol™ is heated to cause material transformation, stiffness is increased by a factor of 4 and the yield strength is increased by a factor of 10. Active mass dampers are already in use. They are generally tuned to the first fundamental frequency of the structure, and they are only effective when the first mode is the dominant vibration mode. Variable stiffness systems use active control to adjust structural stiffness so that resonant modes of a structure are steered away from dominant modes.<sup>1</sup>

SMA smart structures are typically fabricated with reinforced composite materials. SMA reinforced composites use the SMA as the reinforcing fiber, which can be easily embedded into a variety of flight vehicle composite materials and used to control structural response such as static deformation and vibration. Nitinol™ can be embedded in a graphite epoxy matrix. DuPont produces FP fibers for this application also. Active modal modification can be achieved by heating SMA fibers and changing the stiffness of all or portions of a flight control surface. Natural frequencies and mode shapes can be tailored by the fiber volume fraction and number of actuators.<sup>4</sup> Adaptive resonance tuning is achieved using SMA hybrid composite aerodynamic surfaces which are locally stiffened by selectively activating embedded SMA fibers, enabling the surface to attenuate vibration over several activation-dependent frequency ranges. These characteristics can be utilized in a controlled fashion to manipulate dynamic response. SMA's possess actuation, sensing, and control capabilities which can be used to provide adaptability to changing environmental conditions such as loads during ascent. It has been shown (Rogers 1990) that lower order (third through sixth) vibration modes can be successfully altered (first and second modes are more difficult to modify with global actuation but are being worked). Figure 15 shows altered mode shapes. Fibers are activated at the center to change first and second mode shapes.

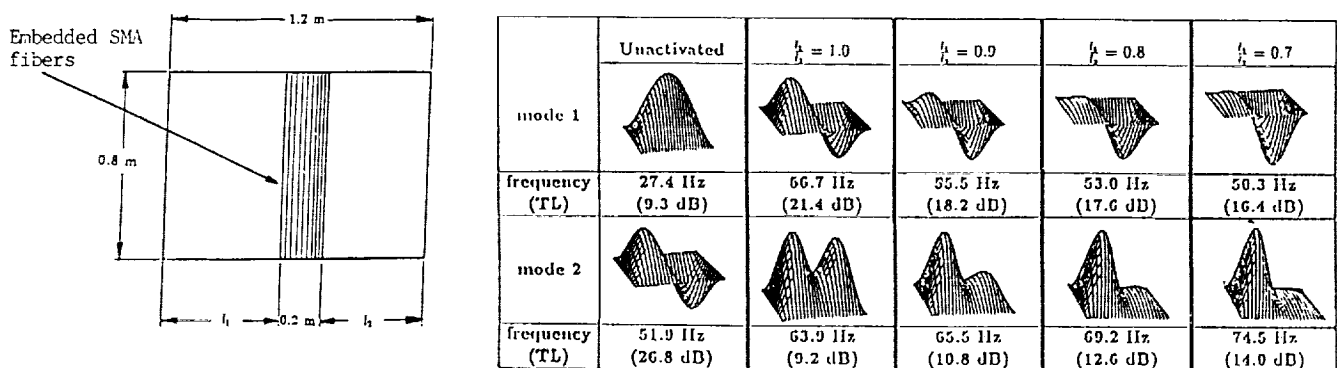


Figure 15. Shape memory alloy fibers for resonance tuning.

Aerospace applications include the Goodyear-developed space antennae. This wire hemisphere of SMA is crumpled into a tight ball less than 5 cm across. When heated above 77 °C, the ball opens up into its original shape, a fully formed antenna. This application has demonstrated the magnitude of deformation possible with SMA's.<sup>5</sup> A wire 30 mil in diameter can generate 75 lb of actuation force. By modulating the heating rate, the degree of control surface deflection can be controlled.

SMA springs as control elements have been used as force and displacement actuators. SMA hybrid composites are a class of materials which combine the strain recovery and stiffness transformation capabilities of SMA fibers with the structural characteristics of advanced composite materials and can produce smart flight control surfaces which can generate substantial aerodynamic forces and control torques. The origin of this concept actually originated from fish fins which have flexible structures that are actuated by contracting muscle fibers contained within a pliable skin. The Naval Warfare Center has used SMA's for adjustable camber in flight control surfaces. The concept employs SMA wires to control the flight of aerodynamic or hydrodynamic vehicles. An operational model has been fabricated and demonstrated. Lift measurements indicated 40 percent higher lift forces than rigid flight control surfaces at the same angles of attack ( $\alpha$ ). Shape memory alloys adjustable camber (SMAAC) control surfaces are a viable method of developing flexible control surfaces with variable camber and  $\alpha$ . The SMAAC control surface produces increased lift at a given  $\alpha$ . The SMAAC concept employs a flexible spring backbone which is activated by contracting SMA wires and is covered by a pliable elastomer skin to produce an adjustable control surface shape. Low aspect ratio swept wings and fins have been studied. Self contained actuators require only electrical leads (Defense Advanced Research Projects Agency sponsored work).<sup>1</sup>

Some A/C programs are nonarticulating flight control surfaces, where the appropriate regions at the edges of the relevant airfoil sections deform in order to provide the aerodynamic control required. There are many programs in progress for smart wings to control dynamic response (figs. 16 and 17). This flight vehicle application features finite element control segments and incorporates sensors, actuators, and microprocessing capabilities. The sensors monitor chosen vehicle and environmental variables. The control strategy synthesizes the desired response by controlling the material characteristics of the actuators in the specific finite element segments.<sup>4</sup>



Figure 16. Use of adaptive truss for wing rib.<sup>3</sup>

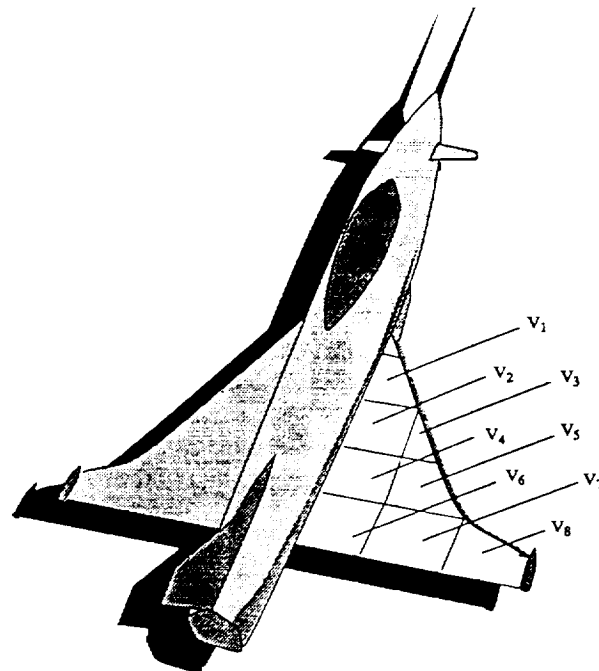


Figure 17. Active control of wing dynamic response using smart materials.<sup>4</sup>

In flight vehicles, the employment of smart materials alleviates the need for the over-design situation based on the worst-case scenario of operating conditions which, of course, results in inferior performance at nominal conditions. The innovative L/V aerodynamic controls could integrate sensing, processing, and actuator functions, and respond autonomously to acceleration flight loads, flutter, buffeting, wind, wind shear, and wind gusts. Larger wind loads could be allowed and launch opportunities increased. Smart skins provide a dynamic interface with the external flight environment and allow all smart components to be embedded in the flight control surfaces, therefore, not affecting the aerodynamics of the surface. This allows the avionics design engineer greater freedom. Optimal control strategies could be employed to tailor the aerodynamic and aeroelastic characteristics of the flight controls to provide maximum control authority augmentation.

For example, a fiber-optic sensing system could instantaneously sense vibration and temperature, which would permit the microprocessor to optimally actuate the ER fluid, magnetostrictive, SMA, and PE domains in the flight control surfaces. The SMA actuators could be used for generating large changes, the PE actuators for changing surface geometries, and the ER and magnetostrictives to control vibration. SMA's allow large changes to geometry (fig. 18). The flight control surface can be designed at the macromechanical level by selection of size, shape, type, number, and spatial distribution of the actuator. Table 6 shows a quantitative comparison of typical smart materials.<sup>7</sup>

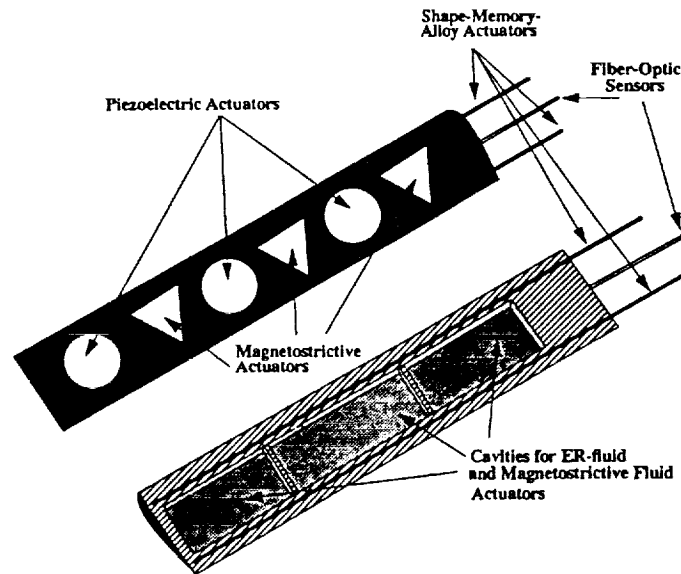


Figure 18. Smart material helicopter rotor blade.

Table 6. Comparison of smart materials.

	PZT G-1195 Piezoceramic	PVDF Piezo Film	PMN-BA Electrostr.	Nitinol™ Shp. Mem.	Terfenol-D™ Magnetostr.
Max. strain (p/m)	300	300	600	20,000 AC	1,800
E (lb/in <sup>2</sup> )×10 <sup>-6</sup>	9	0.3	17	8	7
T max (°C)	360	100	high	45	380
Hysteresis (percent)	10	>10	<1	5	2
Bandwidth	kHz	kHz	kHz	1 Hz	100 Hz
Temp. sen. (percent/°C)	0.05	0.8	0.9		0.3

Cincotta et al. received a patent in May 1992 on an articulated control surface for flight control using SMA's. Beauchamp et al. received a patent in February 1993 on an articulated fin/wing control system using SMA's.<sup>10 11</sup>

## XI. ADVANCED COMPOSITES FOR FLIGHT CONTROLS

NASA's investment of more than \$89 million in the Advanced Composites Technology (ACT) Program, whose goal is "to make composites safe and affordable," has been instrumental in the development of many new flight control surface materials and fabrication techniques. One example of the new composite-part fabrication techniques involves near-net-shape preforms, made by applying textile weaving technologies to carbon or other high-strength fibers. Matrix material, such as low-viscosity epoxy, is then injected into the preform, and the part is cured to a shape requiring minimal machining. Lockheed will use braided textile preforms for braided composite helicopter parts. McDonnell Douglas is using through-the-thickness stitching of multilayer fabric for preforms, with subsequent injection of matrix resin, for major structural parts. By the turn of the century, they hope to certify a 200-passenger A/C with a totally composite wing. The vehicle would be as much as 40 percent composites by weight if used in the fuselage also.<sup>12</sup> Many flight control surface composite materials which have become standard are being superseded.

Kevlar-49™, DuPont's trade name for an aramid fiber (poly(p-phenyleneterephthalamide)) made in China, has a tensile strength of 200 ksi and a strength to weight ratio of 101.8 and has been used on A/C noses and wing L.E.'s. Kevlar-49™ (fig. 19) has the lowest specific gravity and highest tensile strength/weight ratio among current fibers in their class, with superior damage tolerance against impact or other dynamic loadings. Kevlar-49™ fibers do not melt or support combustion, have a very high vibration damping coefficient, are hygroscopic, and can absorb up to 6-percent moisture at

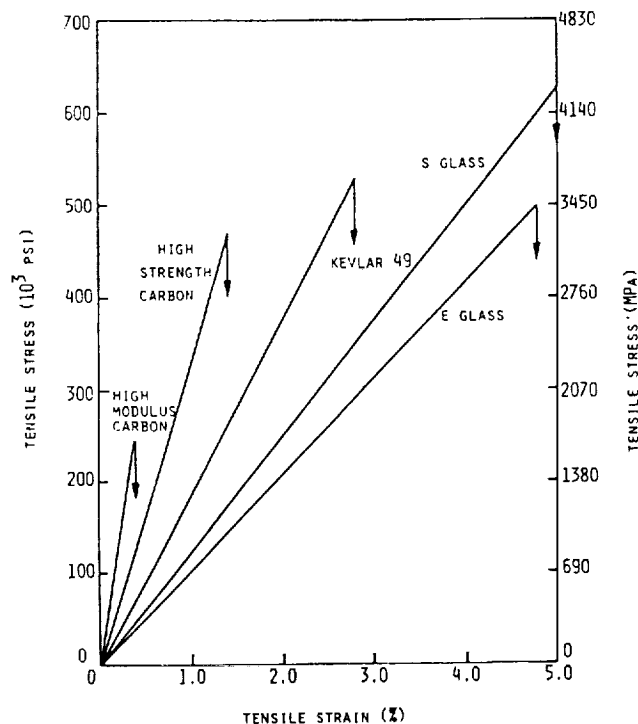


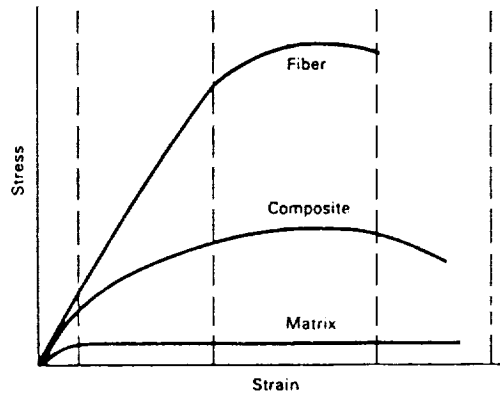
Figure 19. Tensile stress-strain for Kevlar-49™.

100-percent relative humidity and 23 °C, but will start to carbonize at 427 °C.<sup>13</sup> The maximum long-term use temperature for Kevlar-49™ is about 160 °C. Boron fiber-reinforced epoxy skins have been used since 1969 on A/C aerodynamic surfaces such as the F-14 horizontal stabilizer. Carbon/graphite fibers, widely used in aerospace, have tensile moduli of  $150 \times 10^6$  lb/in<sup>2</sup>, very low coefficients of thermal expansion, and high fatigue strengths. Carbon fibers, either alone or in hybridization with Kevlar-49™ fibers, have become the primary material for flight control surfaces, wings, and fuselages (table 7).<sup>13</sup> A second-generation Kevlar™ fiber is Kevlar-149™, which has the highest tensile modulus of all commercially available aramid fibers, and is 40 percent higher than Kevlar-49™.<sup>13</sup> The structural integrity and durability of these components have built up confidence in their performance and prompted much wider use (fig. 20).<sup>14</sup>

Table 7. Composite flight control applications.

Military Aircraft	Component	Material		Overall Weight Savings Over Metal Parts (percent)
F-14 (1969)	Skin on the horizontal stabilizer box	Boron fiber-epoxy		19
F-11	Underwing fairings	Carbon fiber-epoxy		25
F-15 (1975)	Fin, rubber, and stabilizer skins	Boron fiber-epoxy		
F-16 (1977)	Skins on vertical fin box, fin leading edge	Carbon fiber-epoxy		23
F/A-18 (1978)	Wing skins, horizontal and vertical tail-boxes; wing and tail control surfaces, etc.	Carbon fiber-epoxy		35
AV-8B (1982)	Wing skins and sub-structures; forward fuselage; horizontal stabilizer; flaps	Carbon fiber-epoxy		25
Commercial Aircraft	Component	Weight (lb)	Weight Reduction (percent)	Comments
Boeing	Elevator facesheets	98	25	10 units installed in 1980
727	Horizontal stabilizer	204	22	Installed in 1973
737	Wing spoilers	—	37	
756	Ailerons, rudders, elevators, fairings, etc.	3,340 (total)	31	
McDonnell Douglas	Upper rudder	67	26	13 units installed in 1976
DC-10	Vertical stabilizer	834	17	
Lockheed	Aileron	107	23	10 units installed in 1981
L-1011	Vertical stabilizer	622	25	





Material*	Longitudinal modulus ( $E_{11}$ ), in $\times 10^7$ (m $\times 10^7$ )	Transverse modulus ( $E_{22}$ ), in $\times 10^7$ (m $\times 10^7$ )	Shear modulus ( $G_{12}$ ) in $\times 10^7$ (m $\times 10^7$ )
Borsic/aluminum	35 (0.89)	20 (0.51)	10 (0.25)
Boron/epoxy	43 (1.09)	4 (0.10)	1.4 (0.04)
Carbon/epoxy	42 (1.07)	1.9 (0.05)	1.3 (0.03)
Titanium	10 (0.25)	10 (0.25)	4 (0.10)

\* All composites, 50 vol percent fiber.

Figure 20. Composite moduli compared with titanium.

The damping properties of the material represent its ability to reduce the transmission of vibration and the resonance amplitudes of vibration (table 8). Fiber-reinforced composites generally have higher damping factors than metals, and the coefficients of thermal expansion are much less, as can be seen in table 9.<sup>13</sup> Flexural properties, such as flexural strength and modulus, are determined by loading a composite beam specimen of rectangular cross section in either a three-point or four-point bending mode (ASTM test method D790-81). The maximum fiber stress at failure on the tension side of a flexural specimen is considered the flexural strength of the material. Figure 21 shows flexural load deflections of typical unidirectional laminates.<sup>13</sup> The Kevlar-49™ has a highly nonlinear load-deflection curve due to compressive yielding. The flexural modulus is a critical function of the lamina stacking sequence, and therefore will not always correlate with the tensile modulus, which is less dependent on the stacking sequence. In angle-play laminates, a bending moment creates both bending and twisting curvatures which influence the measure of flexural modulus.<sup>13</sup>

Table 8. Damping factors of representative laminates.

Material	Fiber Orientation	Modulus ( $10^6$ lb/in <sup>2</sup> )	Damping factor $\eta$
Mild steel	—	28	0.0017
6061 Al alloy	—	10	0.0009
E-glass-epoxy	0°	5.1	0.0070
Boron-epoxy	0°	26.8	0.0067
Carbon-epoxy	0°	27.4	0.0157
	22.5°	4.7	0.0164
	90°	1.0	0.0319
	[0/22.5/45/90] <sub>s</sub>	10.0	0.0201

Table 9. Coefficients of thermal expansion of representative laminates.

Material	Coefficient of Thermal Expansion, 10 <sup>-6</sup> m/m per °C (10 <sup>-6</sup> in/in per °F)		
	Unidirectional (0°)		Quasi-isotropic
	Longitudinal	Transverse	
S-glass-epoxy	6.3 (3.5)	19.8 (11)	10.8 (6)
Kevlar 49™-epoxy	-3.6 (-2)	54 (30)	-0.9 to 0.9 (-0.5 to 0.5)
Carbon-epoxy			
High modulus	-0.9 (-0.5)	27 (15)	0 to 0.9 (0 to 0.5)
Ultra-high modulus	-1.44 (-0.8)	30.6 (17)	-0.9 to 0.9 (-0.5 to 0.5)
Boron-epoxy	4.5 (2.5)	14.4 (8)	3.6 to 5.4 (2 to 3)
Aluminum		21.6 to 25.2 (12 to 14)	
Steel		10.8 to 18 (6 to 10)	
Epoxy		54 to 90 (30 to 50)	

Note: The fiber content in all composite laminates is 60 percent by volume.

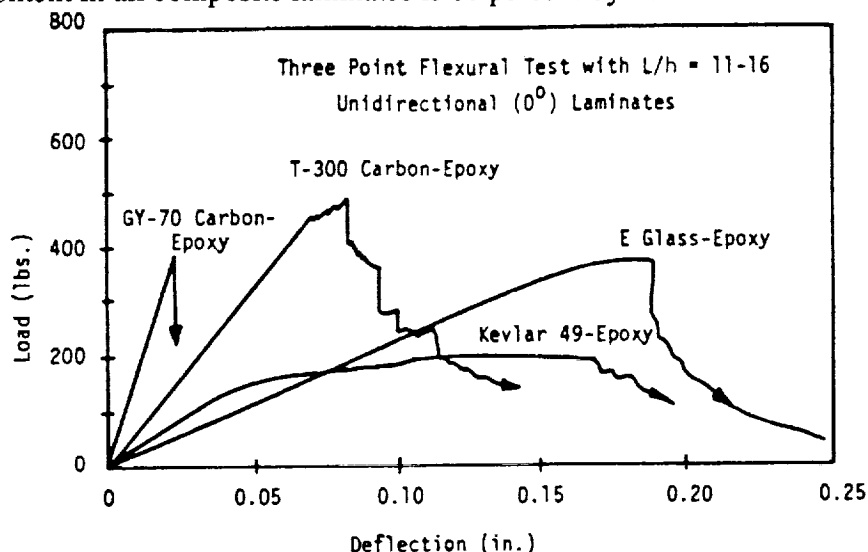


Figure 21. Load deflections for typical 0° unidirectional laminates.

Aerospace applications of structural composites usually use 60 percent fiber volume. Computer methods have been developed to optimized internal fiber arrangements in composite materials for minimum weight and maximum strength.<sup>1</sup> Substantial amounts of carbon and Kevlar-49™ fiber-reinforced composites have been used for some time on A/C flight control surfaces. The Lear Fan 2100 business jet uses over 70-percent carbon and Kevlar-49™ for its structural weight.<sup>13</sup> Helicopter rotor blades have long used fiber-reinforced epoxies, not only for weight reduction, but also for their ability to tailor the dynamic frequencies. The critical flopping and twisting frequencies of the blade are controlled and tuned, not only by the classical methods of mass distribution, but also by varying the type, concentration, and distribution, as well as the orientation, of the fibers along the blade chord length. A

great advantage of composites in helicopter blades is the manufacturing flexibility of the materials. The composite blades are molded into complex airfoil shapes with little or no additional manufacturing costs, while conventional metal blades are limited to shapes that can be extruded, machined, or rolled. Fabrication of large composite parts is done in autoclaves, large variable-pressure ovens for precision curing of epoxy polymers. Composite hydrofoil control flaps of Ti-clad graphite/epoxy are used to withstand critical pressure loadings of 6,300 lb/ft<sup>2</sup>.<sup>15</sup> Polymeric composites such as polyimide or cyanate ester, reinforced by premium carbon fibers, have been used in A/C flight control surfaces. When surface-treated with cold air plasma, the interlaminar shear strength is increased by 60 percent.<sup>16</sup> Hybrid composites use more than one type of fiber and/or more than one matrix.

Significant among high-temperature composites are matrix resins of polyimides and polyphenylquinoxaline with fibers of graphite and Kevlar<sup>TM</sup>. These have been used in supersonic missiles and on fins at Mach 3 and at 800 °F (fig. 22). Weight savings up to 67 percent have been achieved on missile fins. Composites are routinely selected in missile structures for weight reduction, which increases payload capability. Kevlar-49<sup>TM</sup> or S-glass reinforced epoxies have long been used in filament-wound missile motor cases, where the high strength/weight ratios for these materials allow reductions in motor case thickness resulting in additional weight savings. Kevlar-49<sup>TM</sup>, acrylonitrile, allylamine, and "SB1" matrix are high in tensile strength and are thermally stable with good elastic moduli and low density.

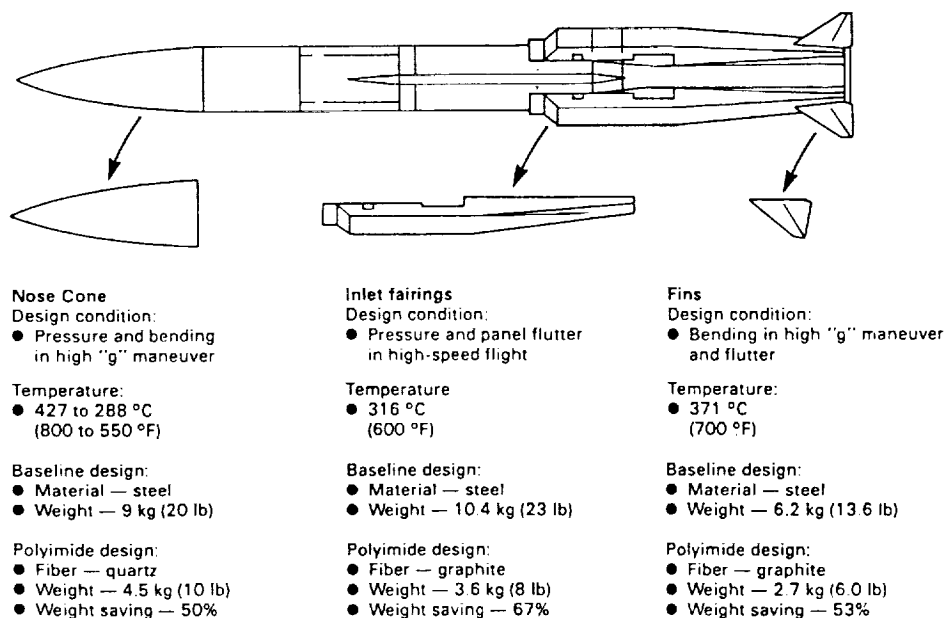


Figure 22. Supersonic missile and fins of polyimide matrix composites.

In many spacecraft (S/C) applications, a major factor in selecting composites is their dimensional stability over a wide temperature range. Many carbon fiber-reinforced epoxy laminates can be designed to produce a coefficient of thermal expansion close to zero. While many aerospace alloys, such as Invar, have comparable coefficients of thermal expansion, the carbon composites have much lower specific gravities and higher strength, as well as a higher stiffness/weight ratio. This unique combination of mechanical properties has led to numerous applications in satellites where temperature ranges of -100 to 100 °C must be accommodated. In the space shuttle, the composites save 3,000 lb per vehicle. Boron fiber-reinforced aluminum tubes are used for the midfuselage truss structure, Al honeycomb in combination with carbon fiber-reinforced epoxy for the payload bay doors, carbon fiber for the remote manipulator arm, and Kevlar-49<sup>TM</sup> for pressure vessels.<sup>17</sup>

Composite flight controls are used on many flight vehicles including the Airbus A310, Lockheed L-1011, McDonnell Douglas DC-10, F-15 (boron/epoxy), and Pegasus. Composite flight control surfaces are required to replace production metal surfaces in fit, form, function, and stiffness, and result in weight reduction. They must meet the fail-safe design criteria for limit flight loads in accordance with the Federal Aviation Administration (FAA) requirements and not degrade in their operating range of  $-54$  to  $82$  °C ( $-65$  to  $180$  °F) or in high humidity conditions. The F-22 A/C and the Pegasus L/V use composite wing designs (Scaled Composites, Inc.). The DC-10 uses honeycomb sandwich skins, graphite/epoxy, and a 4-spar, 13-rib structure for vertical stabilizer and flight controls. Airbus was the first commercial A/C to use composite primary structures. The vertical fin and control surfaces are carbon/epoxy. A well-known benefit of using composites is the elimination of fasteners. Example benefits can include 22-percent weight reduction and 95 parts versus 2,076 parts. Boeing has saved 1,000 lb and achieved a smoother, drag-reducing skin surface by using carbon fiber/epoxy composites on the primary structural components, the 47-ft tall vertical tailfin, and the horizontal stabilizers of the B-777 transport. This is the first American passenger airplane to have an all composite empennage.

The L-1011 uses graphite/epoxies in the vertical fin and flight controls. The L-1011 ailerons are a wedge-shaped, one-cell, box configuration consisting of a front spar, a rear spar, upper and lower covers, reinforcing ribs, L.E. shrouds, end fairings, T.E. wedge, shroud supports, and feedback, hinge, and actuator fittings. Inboard ailerons are located between the outboard and inboard flaps on each wing as shown in figure 23. Figure 24 shows a typical L/V flight control surface for comparison. Each aileron is 92 inches in span, 50 inches in chord, and 10 inches in thickness.<sup>13</sup>

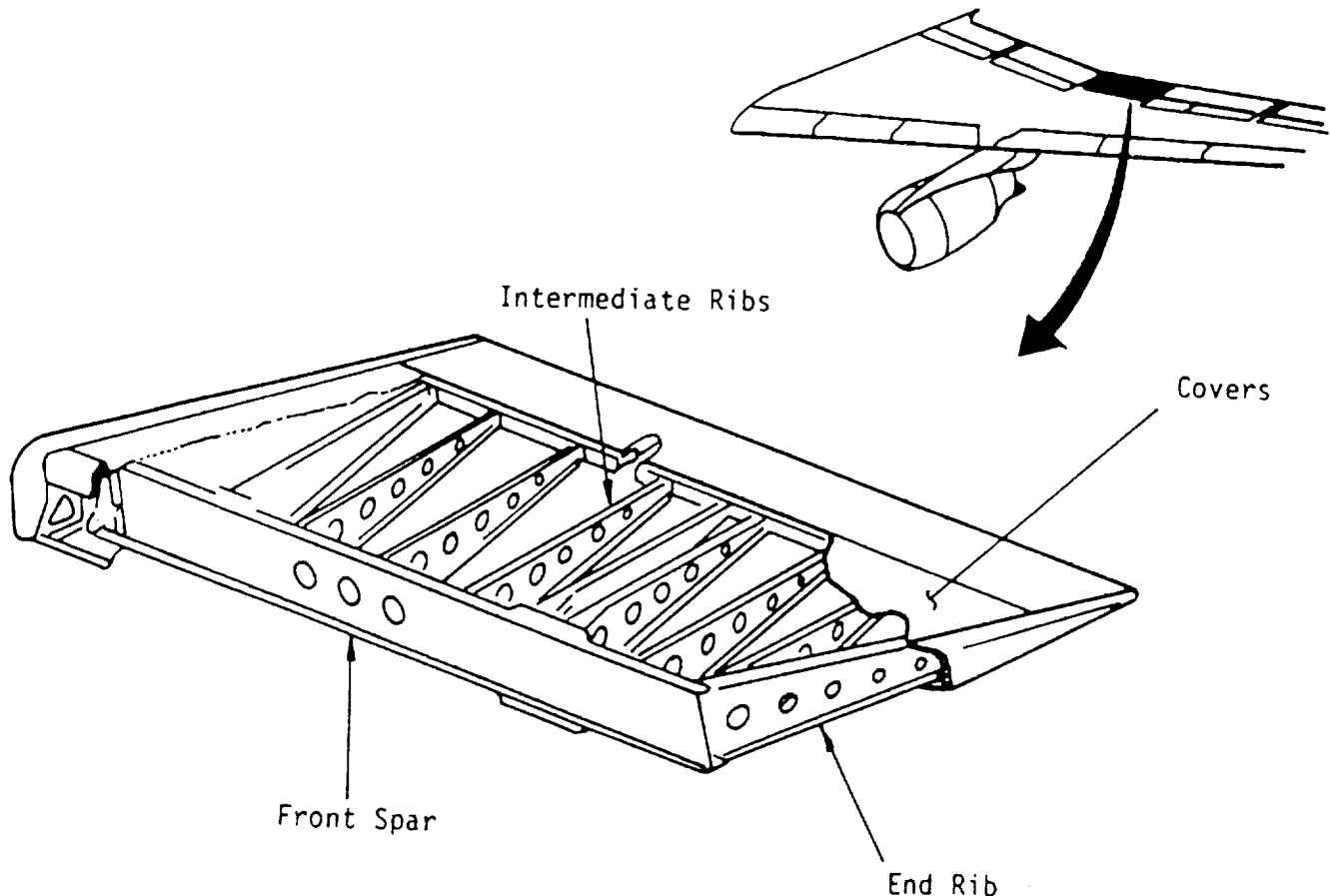


Figure 23. Construction of Lockheed L-1011 composite aileron.

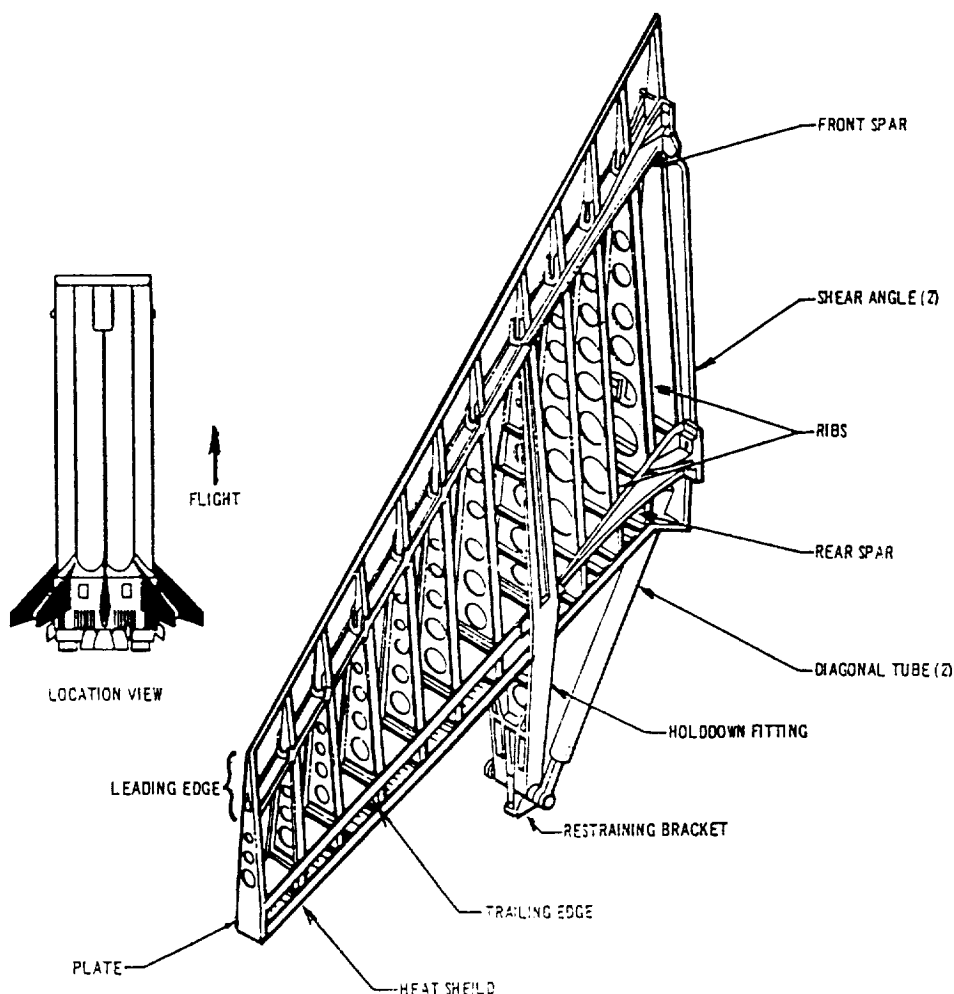


Figure 24. Typical L/V aerodynamic surface (Saturn IB).

The following were selected for principal structural components of the composite ailerons. Upper and lower covers: T-300 carbon fiber epoxy sandwich construction of three layers; laminate configuration of 45/0/-45/syntactic core/-45/0/45 with the 0° plies oriented in the spanwise direction; near main rib and at ends of each cover five plies of T-300 oriented in the chordwise direction. Front spar: constant-thickness channel section of 45/0/-45/90/0 laminate; zero plies front spar in spanwise direction. Main ribs: used at three hinge or actuator locations for transferring loads from the fittings to the aileron covers and spars. In the aileron assembly, the upper cover, all ribs, and two spars are permanently fastened with titanium screws and stainless steel collars. The lower covers are removable. All carbon-epoxy parts are painted with a urethane coat. These composite flight control surfaces are 23-percent lighter and contain 50-percent fewer parts (table 10). Table 11 gives a summary of ground tests.<sup>13</sup>

Table 10. Comparison of composite and metal flight control surfaces.

	Composite	Aluminum
Weight (lb)	100.1	140.4
Number of ribs	10	18
Number of parts	205	398
Number of fasteners	2,574	5,253

Table 11. Composite flight control surface ground tests.

Vibration in the flapping mode	Resonance frequencies comparable to those of metal ailerons
Vibration in the torsional mode	Resonance frequencies comparable to those of metal ailerons
Chordwise static bending stiffness	Composite ailerons 27 percent less stiff than metal ailerons
Static torsional stiffness	Comparable to metal ailerons
Static loading	124 percent design ultimate load without failure at 12° down-aileron positions  139 percent design ultimate load at 20° up-aileron positions with postbuckling of the hinge and backup rib webs
Impact loading to cause visible damage at four locations followed by one lifetime flight-by-flight fatigue loading	Slight growth of damage (caused by impact loading) during the fatigue cycling
Simulated lightning followed by static loading	Burn-through and delamination over a small area; however, no evidence of growth of this damage during static testing

The B-777 composite consists of a high-strength carbon fiber containing toughened epoxy resin supplied by Toray Industries, headquartered in Tokyo. This Toray composite material was demonstrated to NASA engineers. The material's damage resistance is seven times that of conventional composites. The Toray flight control surface and empennage composite material, designated P3202, dents like metal when damaged so that visual inspection of flight control surfaces would be 100-percent reliable. P3202 contains Toray's own T-800 graphite carbon fiber in a matrix of 3900-2 epoxy. Epoxy is a thermosetting resin which, once cured, cannot be remelted and tends to be brittle. The P3202 gets its toughness from inherently more rubbery microparticles of thermoplastic material introduced between the thermo setting prepreg ply layers.<sup>12</sup>

## XII. CARBON-CARBON COMPOSITES

Carbon-carbon composites (CCC's) are the most highly developed of the ceramic-ceramic composites, consist of reinforcing fibrous carbon substrate in a carbonaceous matrix, and are made in a variety of forms (fig. 25) with tensile moduli up to  $100 \times 10^6$  lb/in<sup>2</sup>.<sup>18</sup> CCC's were developed to meet aerospace material needs of structural integrity at high temperature in excess of 5,000 °F and have been used extensively in missiles, exhaust nozzle throats and flaps, turbine blades, heat shields, reentry vehicles, and soon, pistons for internal combustion engines. A CCC piston for use in reciprocating engines has been successfully tested at LaRC, and a U.S. patent has been issued. 3-D CCC is an attractive material for nozzle throat and exit areas. 3-D weaving technology, as developed by Aerospatiale

and Brochier, S.A. in France, has been licensed and transferred to U.S. firms because 3-D CCC components are replacing the weaker two-dimensional materials. CCC's are used on the space shuttle because of their high strength levels at temperatures over 1,650 °C and stiffness to resist flight loads and large thermal gradients. Ceramic matrix composites, slated for use on the high speed civil transport (HSCT) engines, consist of inorganics such as silicon nitride or silicon carbide reinforced with high-strength ceramic fibers.

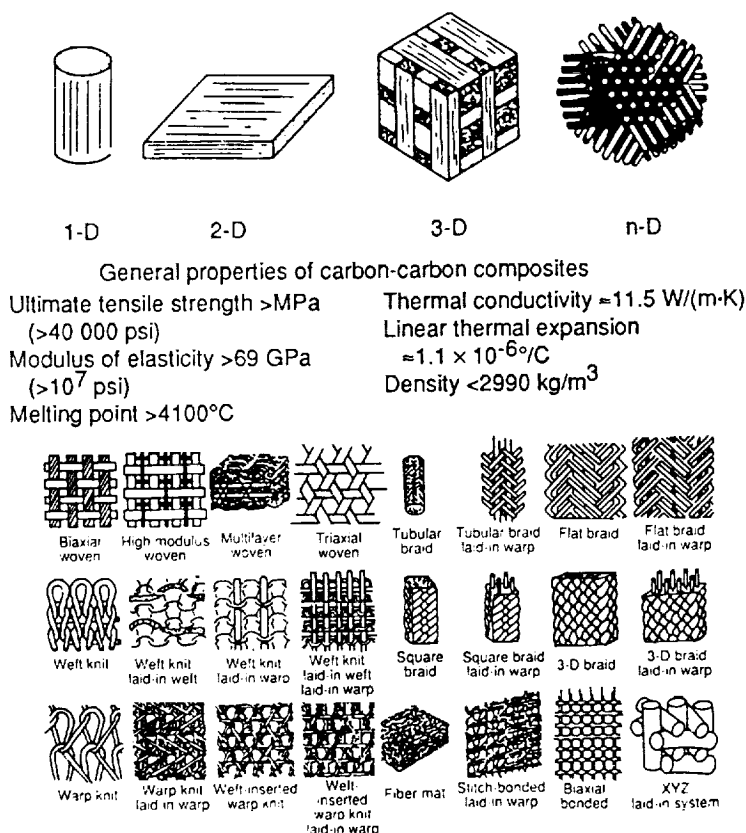


Figure 25. General properties and weaves of carbon-carbon composites.

Carbon fibers are 93- to 95-percent carbon, whereas the higher modulus graphite fibers are 99+ percent carbon. Graphite filaments have very high strengths and moduli which remain constant at high temperatures. Graphite fibers are the stiffest fibers known and approximately five times more rigid than steel. The fibers themselves are composites; only part of the carbon present has been converted to graphite in tiny crystalline platelets specially oriented with respect to the fiber axis. These are used extensively in the missile and A/C industry (fig. 26), hence are directly applicable to L/V flight controls.

CCC's have matured considerably since first used on S/C. The key to these advances is improved oxidation-resistant materials for atmospheric use at high temperatures. Although CCC's can withstand temperatures >3,000 °C in a vacuum or inert atmosphere, they oxidize when in an oxygen atmosphere at 600 °C. To use CCC parts in an oxidizing atmosphere, they must be compounded with materials that produce oxidation-protective coatings, or must be coated and sealed. On the space shuttle, the CCC L.E.'s and nose cap are converted to silicon carbide in a high temperature diffusion-coating process. Improvements are being developed for oxidation protection of CCC components on the space shuttle. Figure 27 shows three levels of CCC strength efficiency. The first, labeled space shuttle material, is the strength level of reusable CC (RCC).<sup>18</sup>

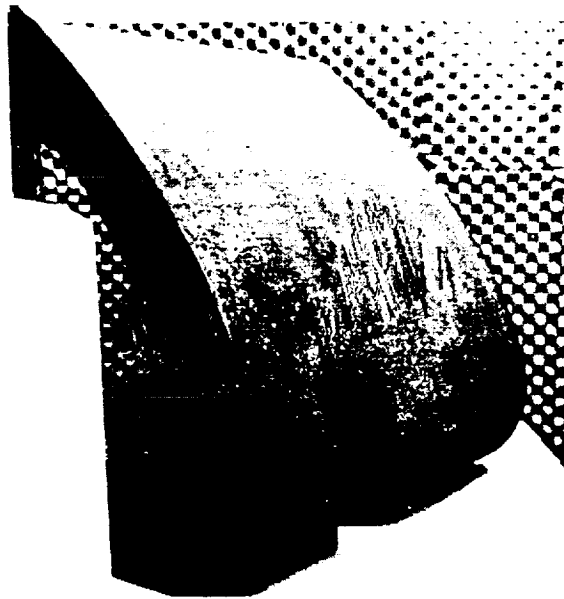


Figure 26. Space shuttle orbiter CCC wing L.E.

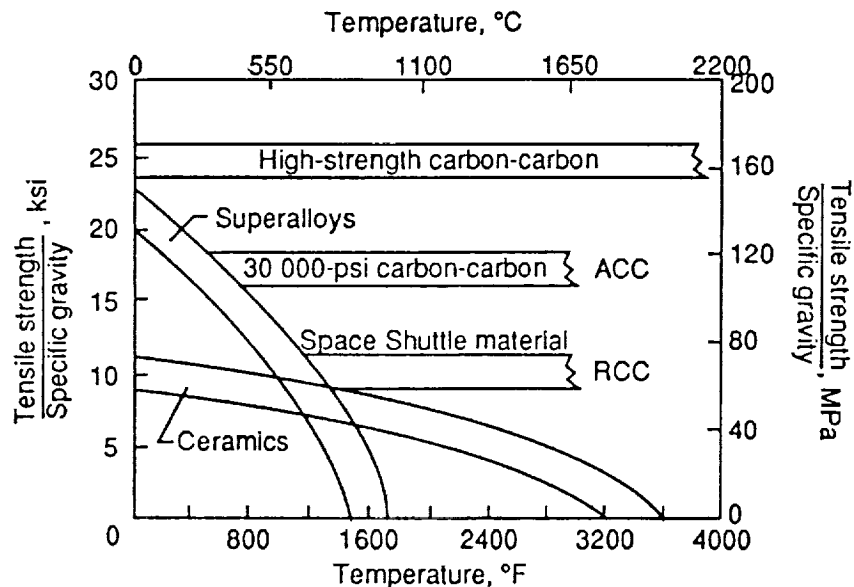


Figure 27. Carbon-carbon strength-to-density ratios.

Reusable CCC's are being used for fin L.E.'s on missiles, wind tunnel test articles, and many flight vehicles including the National Aerospace Plane (NASP). Shuttle wing L.E.'s and the nose withstand 1,540 °C. The L.E.'s contain 22 CCC airfoil panels and 22 sealing strips of CCC. Reusable CCC on the space shuttle is protected from oxidation by a two-layer coating of a porous silicon carbide (Si-C) inner layer sealed with Si-O<sub>2</sub> and an outer coating of alkali silicate glass filled with Si-C particulate. Si-C fiber has been used as a reinforcement in ceramics for L.E.'s of wings and control surfaces of hypersonic flight vehicles. Reusable CCC's have good strength up to temperatures of 2,760 °C.<sup>18</sup>

CCC has been chosen for flight control surfaces on the NASP. Continuous graphite fibers are combined in a 3-D geometry with a graphite matrix to create the CCC for the NASP wing L.E.'s and for missile nose cones.<sup>17</sup> LaRC has sponsored this development effort. LTV Corp. is developing the CCC



eleven control surfaces, and CCC will accommodate the 1,930 °C temperatures on the NASP wing L.E.'s. The European spaceplane, Hermes, is also using CCC for the L.E.'s.<sup>18</sup> Carbon-fiber reinforced plastic (CFR), which is used in the fin box for the Airbus A300/A310, has lowered total manufacturing costs by 85 percent. Shell assemblies, spars, and ribs of the fin box are stiffened by a modular grid (fig. 28).<sup>15</sup> Each module is an Al core, around which the prepreg carbon fiber-reinforced plastic is wrapped. The skin is also laid up mechanically with reinforcements in the spar and rib areas.

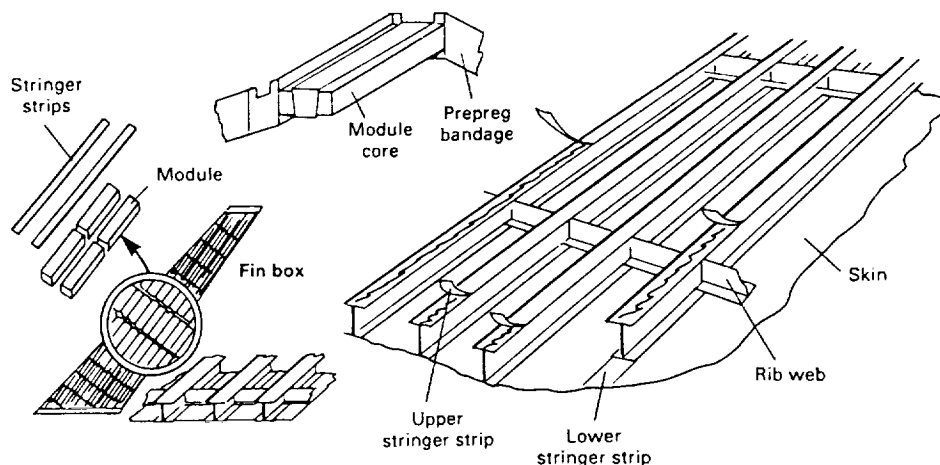


Figure 28. Carbon-fiber reinforced Airbus fin box.

Advanced CCC's (ACC's), which are twice as strong (fig. 27), have been selected as the material to be used for the flight control surfaces, body flaps, chines, and fin L.E.'s of the NASA Personnel Launch System, the HL-20. This ACC will withstand up to 3,300 °F. Carbon/boron nitride composite made from carbon fibers in a boron nitride matrix which can withstand temperatures twice as high as CCC's has been developed by the University of Illinois under Advanced Projects Research Agency and Naval Research support.

### XIII. INTERMETALLICS

Intermetallics have a characteristic ordered crystal structure leading to high resistance to deformation and melting points > 1,650 °C. Ni-Al alloys have been used in 1,380 K temperature ranges on flight vehicle engines. Several intermetallics possess strength up to three times greater than that found in Ni<sub>3</sub>-Al at comparable temperatures (table 12).<sup>9</sup>

The Al-Li alloy has much aerospace usage, including the Centaur and Titan payload adapter, due to the 10-percent decrease in density and 10-percent increase in elastic modulus. Alcoa has recently developed a special new Al-Li, the C-155, for flight vehicle stabilizers and flight controls (*Aviation Week*, January 24, 1994). Lockheed's large-scale tests of Al-Li alloys have shown service life to be three to five times greater than conventional 2124-T851 Al plate. Vought Aircraft Company has explored various forms of laminated intermetallic. The fault of the intermetallic at ambient temperature is low ductility. Nb-Ti-Al is good at 1,700 °C but brittle at room temperature. Ordered intermetallics (fig. 29),<sup>9</sup> based on aluminides and silicides, have superior oxidation and corrosion resistance, good high-temperature strength and stiffness, and low density, but plagued by brittle fracture and poor ductility at ambient temperature. Examples are: Ti-Al<sub>3</sub> (3.4g/cm<sup>3</sup>), Ti<sub>3</sub>-Al (4.2g/cm<sup>3</sup>), and Ti-Al-C. Titanium alloys such as  $\alpha$ ,  $\beta$  alloys, e.g., Ti-6Al-9V and metastable  $\beta$  alloys, e.g., Ti-10V-2Fe-3Al are used at temperatures over 500 °C.<sup>13</sup>

Table 12. Characteristics of selected intermetallics.

Intermetallic Compound	Crystal Structure (Ordered)	Melting Point °C (°F)	Density g/cm <sup>3</sup> (lb/in <sup>3</sup> )	Young's Modulus GPa (10 <sup>3</sup> lb/in <sup>2</sup> )
Ni <sub>3</sub> -Al	face centered cubic	1,390 (2,530)	7.50 (0.274)	178.5 (25.9)
Ni-Al	body centered cubic	1,640 (2,980)	5.86 (0.214)	294.2 (42.7)
Fe <sub>3</sub> -Al	body centered cubic	1,540 (2,800)	6.72 (0.245)	140.0 (20.4)
Fe-Al	body centered cubic	1,250 (2,280)	5.56 (0.203)	260.4 (37.8)
Ti <sub>3</sub> -Al	hexagonal close packaged	1,600 (2,910)	4.20 (0.153)	144.7 (21.0)
Ti-Al	tetragonal	1,460 (2,660)	3.91 (0.143)	175.6 (25.5)
Al <sub>3</sub> -Ti	tetragonal	1,350 (2,460)	3.40 (0.124)	
Nb <sub>2</sub> -Be <sub>17</sub>	rhombohedral	1,705 (3,100)	3.28 (0.120)	296.3 (43.0)
Al <sub>3</sub> -Nb	tetragonal	1,600 (2,910)	4.54 (0.166)	

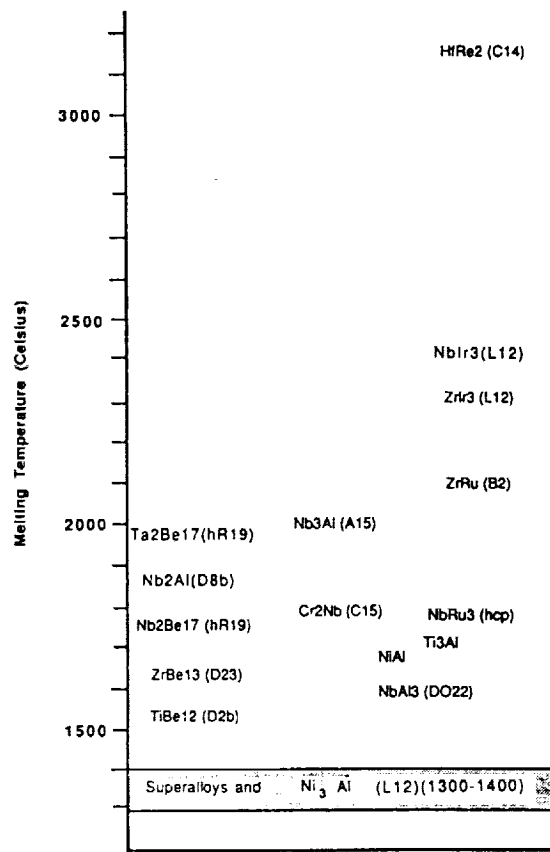


Figure 29. Melting points of example intermetallics compared to superalloys.

Intermetallics have been improved in ductility by incorporating ductile particles of other metals such as Nb, e.g., Ti-14Al-21Nb ( $\alpha$ -2) which can be used up to 980 °C, and  $\beta$  stabilizers such as Nb, V, and Mo have improved the Ti<sub>3</sub>-Al alloys with 10 to 25 percent Nb addition to promote ductility, thus allowing the fabrication of complex shapes, Ti-24Al-9Nb-2V, Ti-14Al-21Nb ( $\alpha$ -2), Ti-14Al-19Nb-3V-2Mo(super  $\alpha$ -2), and Ti-33Al-6Nb-1.4Ta( $\gamma$ ) being among the best. Ti-6Al-4V has UTS of  $200 \times 10^3$  lb/in<sup>2</sup>. Tensile strength and ductility of Ti-6Al-TiC is greatly affected by microstructure. Fast cooling rates in formation generate higher strength. Adding third elements, such as 2 percent by weight of Mn or V (Ti-30Al-20V) to Ti-Al-based alloys improves strength and ductility. This improvement is recognized as the result of refinement of the microstructure of grains, which reduces the slip length of dislocations that correspond to increased strength and ductility.

Recent advances in material science have shown that Ti-Al-base intermetallics can be used as high temperature aerospace airframe structural material.<sup>16</sup> They exhibit good stiffness combined with adequate creep and oxidation resistance at temperatures of 1,000 °C. An advantage with Ti intermetallics, e.g., Ti-6Al-4V, is the relatively simple application of superplastic forming and diffusion bonding (fig. 30) which allows forming and welding in one step. Aluminum alloys do not exhibit superplastic properties following a conventional production technique. Many titanium aluminides have been slated to be used in the NASP, and figure 31 shows their comparison with composites.<sup>9</sup>

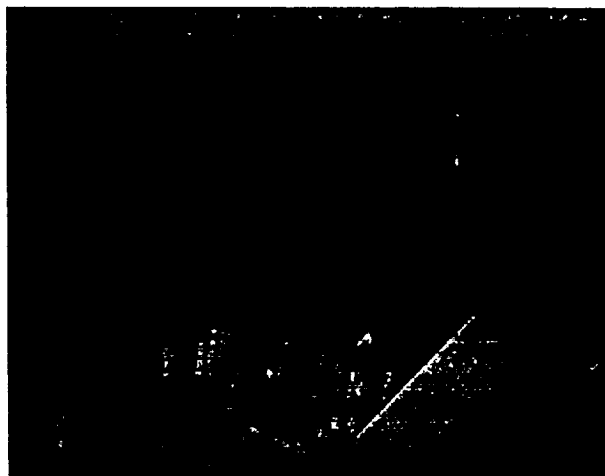
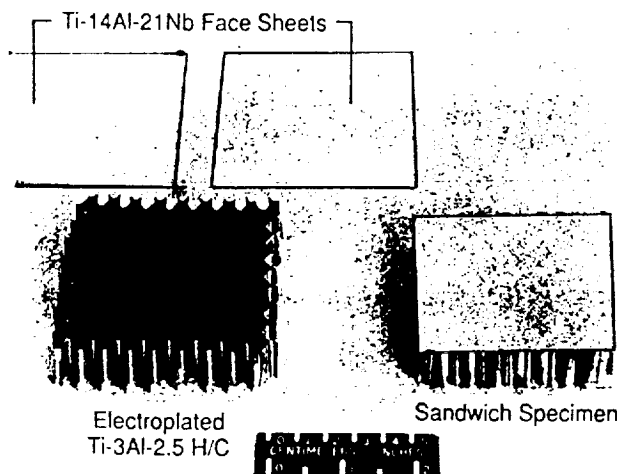


Figure 30. Ti<sub>3</sub>-Al honeycomb structure using diffusion bonding.

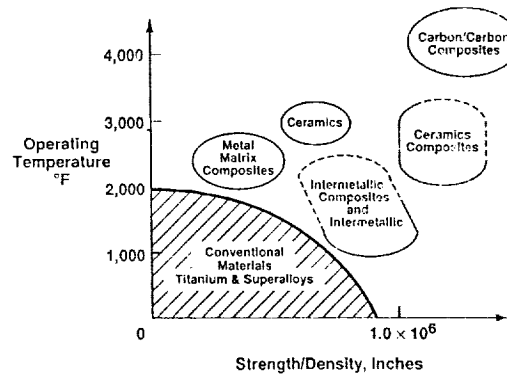


Figure 31. Comparison of intermetallics and composites.

As a result of extensive development programs in both the U.S. and Russia, the intermetallic titanium aluminides, both in composite and monolithic configurations, have significant flight vehicle usage.<sup>9</sup> Since materials are the main driver for the HSCT airframe, NASA is developing a new generation of intermetallic matrix composites for the HSCT. LaRC is researching the prevention of oxidation and embrittlement in Ti-Al intermetallics by the use of a 10- $\mu$ m thick Al-Si-B<sub>x</sub> coating. Intermetallics are known for excellent high-temperature properties, and their composites are excellent candidate materials for flight control surfaces of hypersonic/supersonic vehicles, including the L/V application considered in this paper.

#### XIV. METAL MATRIX COMPOSITES

While conventional composites have many proven applications in flight vehicle control surfaces, they can suffer from fatigue loads at very high temperatures. Typical upper temperature limits on conventional composites are 800 °F. Boron fibers offer excellent resistance to buckling and high compressive strength in addition to extremely high tensile moduli, but they are temperature limited. The metal matrix composite (MMC) has been created to solve this problem. MMC's offer high electrical and thermal conductivity in combination with mechanical strength.

MMC materials benefit from property synergisms which offer greater strength and stiffness, higher temperature capability, lower weight, and better fatigue behavior and wear resistance than the polymer matrices. MMC's can also have strength/weight ratios higher than those of intermetallics and can offer 60-percent savings in weight while still retaining key properties. In the last decade, there has been accelerated research in MMC development, because materials with high strength/weight ratios and high temperature capability are needed for hypersonic flight vehicles. MMC's, based on the principle that the sum is greater than the parts, offer revolutionary new choices in material selection for innovative flight control surfaces. Tailoring the properties of MMC's to specific applications has motivated extended research over the past two decades.<sup>14</sup> New technology has allowed the manufacture of a plethora of new MMC's that have superior properties to their monolithic counterparts and are being used with increasing frequency in aerospace applications.<sup>9</sup>

The advantages of reinforcing metals with ceramic particle to produce MMC's are well known. New generations of MMC's have been produced with enhanced elevated temperature properties and casting, extruding, and forging capability. Aluminum oxide has excellent strength retention up to 1,370 °C. The modulus of metals is an order of magnitude higher than that of polymers (tables 13 and 14).<sup>13</sup>

Table 13. Typical reinforcements used in metal matrix composites.

Reinforcement	Manufacture (Designation)	Form Mono/Tow	Diameter $\mu\text{m}$ (mils)	Strength GPa (ksi)	Modulus GPa (msi)	Elong. Ult percent	Density $\text{g/cm}^3$ (lb/in <sup>3</sup> )	CTE $\text{p/m/K}$	Thermal Cond. (W/mK)	Cost-\$/lb	Production Status (lb/yr)
Tungsten		Mono.	variable	2.41 (350) variable†	406 (59)	†high-var.	19.30	5		200	Special order
Molybdenum		Mono.	variable	1.03 (150) variable	365 (53)	high-var.	10.20	5.8		200	Special order
Carbon-pitch	Amoco-Thor.-P55	Tow	10, 11	1.9/1.72 (275/250)†	380 to 415 (55/60)†	0.50	2.00	-1.3	120/110†		Commercially available in limited quantities
	" Thornel-P75	Tow	10	2.1 to 1.9 (300 to 275)†	520 (75)	0.40	2.00	-1.4	185		"
	" Thornel-P100	Tow	10	2.2 (325)	724 (105)	0.31	2.15	-1.45	520		"
	" Thornel-P120	Tow	10	2.2 (325)	827 (120)	0.27	2.18	-1.45	640		"
	DuPont-E-55	Tow	9.5	3.2 (465)	378 (55)	0.74	2.14				"
	DuPont-E-75	Tow	9.4	3.1 (450)	516 (75)	0.56	2.16				"
	DuPont-E-105	Tow	9.3	3.3 (480)	724 (105)	0.55	2.17				"
	DuPont-E-120	Tow	9.2	3.4 (500)	894 (120)	0.55	2.19				"
	DuPont-E-130	Tow	9.2	3.9 (570)	894 (130)	0.55	2.19				"
	Tonen-HM	Tow	9.7	2.96 (430)	489 (70)	0.61	2.14			20	Commercial
	Tonen-UHM	Tow	9.7	2.96 (430)	699 (100)	0.43	2.17				"
	Mitsubishi-K133	Tow	10	2.19 (314)	447 (64)	0.53	2.08				"
	" Dialed-K135	Tow	10	2.58 (371)	553 (79)	0.47	2.10				"
	" Dialed-K137	Tow	10	2.70 (386)	650 (93)	0.42	2.12				"
	" Dialed-K139	Tow	10	2.79 (400)	747 (107)	0.37	2.14				"
	Hercules IM7	Tow	5	5.31 (770)	301 (43.6)	1.81	1.78				"
Boron	Textron	Mono.	100 and 140	3.52 (510)	400 (58)	0.89	2.60	4.5		600	30,000
Silicon carbide Si-C	Textron	Mono.	75 and 140	3.79 (543)	400 (59)	0.94	3.00	4.2	200	2,500 to 5,000	†1,000 S.T.F.O.
	B.P.-Sigma DuPont-	Mono.	100 30	3.45 (500) 1.17 (170)	414 (60) 379 (55)	0.83 0.31	3.10 3.20	4.2 4.2	200 ~200		†Experimental Experimental
Alumina	DuPont-FP	Tow	20	1.59 (230)	379 (55)	0.42	4.00	5.6		200	500
	PRD-166	Tow	20	2.28 (330)	379 (55)	0.60	4.20	6.8		300	~500
	Sumitomo 85 percent Alumina	Tow	17	1.79 (280)	207 (30)	0.93	4.00	4.5		300	50,000
	3M-Alpha Alumina	Tow	10 to 20	~2.06 to 2.76 (300 to 400)	379 (55)	0.55 to 0.73	0.40				Experimental
	Saphikon	Mono.	75 to 150	2.07 (300)	448 (65)	0.46	4.00			100,000	Experimental

Table 14. Mechanical properties of some metal matrix composites.

Material	Specific Gravity	Tensile Modulus, GPa (Gsi)	Yield Strength, MPa (ksi)	UTS, MPa (ksi)	Elongation percent	CTE $10^{-6}/^{\circ}\text{C}$	Melting point, $^{\circ}\text{C}$
Aluminum alloys:							
2024-T6	2.78	70 (10.1)	468.9 (68)	579.3 (84)	11	23.2	
6061-T6	2.70	70 (10.1)	275.9 (40)	310.3 (45)	17	23.6	
7075-T6	2.80	70 (10.1)	503.5 (73)	572.4 (83)	11	23.6	
8009	2.92	88 (12.7)	407 (59)	448 (64.9)	17	23.5	
380 (as cast)	2.71	70 (10.1)	165.5 (24)	331 (48)	4	—	540
Titanium alloys:							
Ti-6Al-4V (solution treated and aged)	4.43	110 (16)	1,068 (155)	1,171 (170)	8	9.5	1,650
Magnesium alloys:							
AZ91A	1.81	45 (6.5)	158.6 (23)	234.5 (34)	3	26	650
Zinc-aluminum alloys:							
ZA-27 (pressure die-cast)	5	78 (11.3)	370 (43.6)	425 (61.6)	3	26	375

In the MMC, the matrix is a key element which is chosen to transfer stresses between the fibers, providing a barrier against an adverse environment, and protecting the surface of the fibers from mechanical abrasion (fig. 32). The matrix plays a minor role in the tensile load-carrying capacity of a composite structure. However, selection of a matrix has a major influence on the interlaminar shear as well as the in-plane shear properties. Properties parallel to the fiber direction are dominated by the fiber, while those perpendicular to the fiber are dominated by the matrix. Therefore, the plies, orientation, and location are carefully designed. The interlaminar shear strength is an important design consideration for bending loads, whereas the in-plane shear strength is important under torsional loads. The matrix provides lateral support against the possibility of fiber buckling under compression loading, thus influencing to some extent the compressive strength. The interaction between fibers and matrix is also important in designing damage-tolerant structures. The metallic matrices have been selected for high temperature applications, with Al, Ti, and Mg being the most common. These metallic matrix materials require high modulus fibers because their own moduli are high,  $10 \times 10^6$ ,  $16 \times 10^6$ , and  $6.5 \times 10^6$  lb/in<sup>2</sup>, respectively.<sup>15</sup> These are combined with boron, silicon, and graphite. Intermetallic aluminides and silicates are attractive matrix materials due to their resistance to high temperature oxidation. The service temperature of a composite depends on the melting point of the matrix material. MMC's can be used in temperature ranges from cryogenic to 5,000 °F.<sup>15</sup>

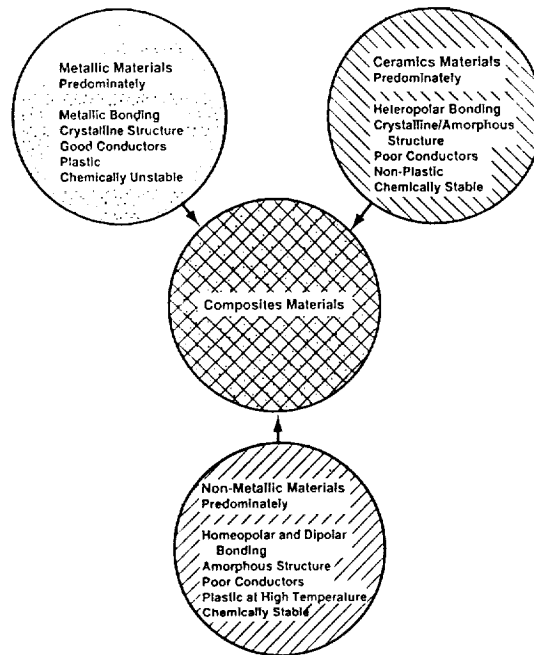


Figure 32. Composite groups.

The reinforcing materials supply the basic strength of the MMC. They can, however, also conduct heat or electricity. If a reinforcement is to improve the strength of a given matrix, it must be both stronger and stiffer than the matrix. Developments of new filaments and whiskers give the engineer freedom to design the material to suit the needs. Chemical interactions between fibers and matrix components and interdiffusional phenomena must be considered to prevent fiber weakening, coarsening, or dissolution. MMC reinforcements include continuous or discontinuous filaments, whiskers or particulates, randomly oriented or aligned, and dispersion-strengthened, continuous, or eutectic phases. The dimensions of the reinforcements can vary from the submicrometer whiskers in situ composites to fibers of 100  $\mu\text{m}$  diameter.<sup>20</sup> Ceramic fibers are notable for their high-temperature applications in metal and ceramic matrix composites. Their melting points are close to 3,000  $^{\circ}\text{C}$ . Much of the recent work on MMC's is based on silicon carbide whiskers or particulates. Fibers are the most important class of reinforcements due to their ability to transfer strength to matrix materials. Table 15 shows the desirable characteristics of a reinforcing fiber.<sup>9</sup> Among fibers which have been used in the A/C industry because of high temperature capability are carbon and graphite used to reinforce Al. Figure 33 shows how the Si-C MMC's compare to the intermetallics.<sup>9</sup>

Table 15. Desirable characteristics of reinforcing fiber.

1. Compatible coefficient of thermal expansion (CTE) with the matrix
2. Chemical compatibility with the matrix even after extended elevated temperature exposures
3. Low density
4. High modulus of elasticity
5. High strength at elevated temperature
6. Good oxidation resistance
7. 50 to 250  $\mu\text{m}$  diameter continuous monofilament
8. Mass production feasibility (including affordable cost).

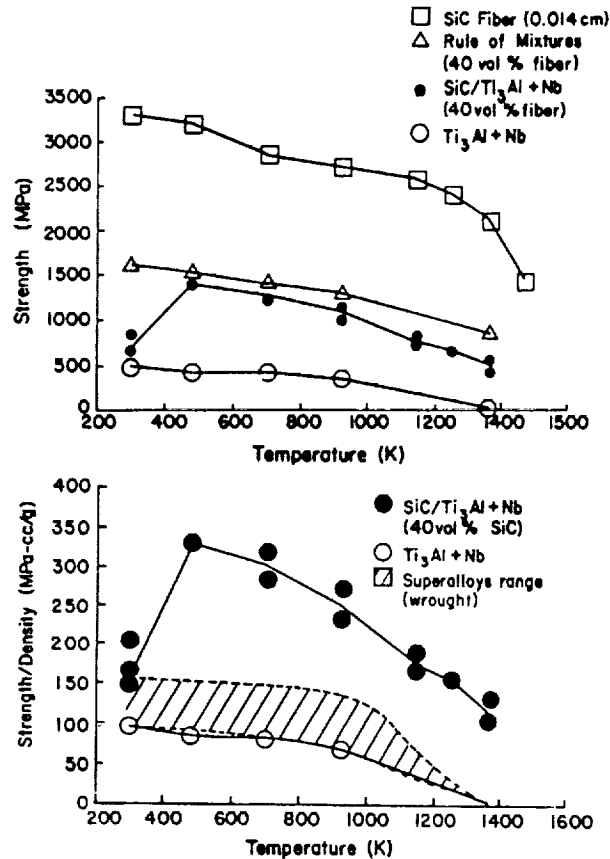


Figure 33. Comparison of metal matrix composite and corresponding intermetallic.

In comparison to the intermetallics, the high cyclic fatigue strength of the MMC is superior, and they possess the advantage of high strength/weight ratio and designability beneficial to aerospace vehicles. Boron-aluminide composite is a MMC which has high strength/weight ratio, stiffness-to-density ratio, excellent compression strength, and is used on the space shuttle. Composite laminated plates and stiffened panels are typically used on flight vehicles. The materials can be aeroelastically tailored for vibration control.<sup>16</sup> The dynamic behaviors, including natural frequencies, mode shapes, and specific damping can be designed by means of changing the orientation of the layers (e.g., 0°, 90°, +45°, -45°, etc.) and the order and numbers (e.g., 1 to 30) of the layers. Strain energy is a convenient parameter to use in defining the damping of a composite. It has been used in damping analysis of fiber reinforced composites. Approaches for damping analysis include modal strain energy, complex eigenvalue method, and direct frequency response.<sup>9</sup> Figure 34 shows 238 nodes, 714° of freedom, 312 composite bars, 152 metallic bars, 99 metallic half web elements, 209 composite half web elements, 8 metallic triangular elements, and 18 composite triangular elements.<sup>16</sup>

MMC's are increasingly used in flight vehicle primary structures which are subjected to severe loading and environment, and would be well suited for L/V flight control surfaces. Lockheed has used Textron's MMC's for vertical stabilizer aerodynamic surfaces. MMC missile fins have been successfully tested.<sup>17</sup> For the application considered in this paper, the best type of continuous reinforcement fibers for intermetallic titanium aluminides are Si-C and Al<sub>2</sub>O<sub>3</sub>. Of all the composite materials surveyed in this research effort, the MMC is best suited for flight control applications on L/V's and hypersonic A/C.





has yet emerged. Si-C is apparently far from ideal, as the reaction layer both forms relatively quickly and has a markedly deleterious effect on composite properties. However, Si-C is the most readily available of the candidate long fiber reinforcements, which are needed for good creep resistance. This has resulted in production of coated Si-C fibers that delay or prevent the deleterious interfacial reaction. Several techniques are available for deposition of thin coatings on long fibers, including chemical vapor and physical vapor deposition.<sup>21</sup>

At the heart of the TMC is a continuous Si-C fiber that reinforces the Ti matrix. Textron, the only U.S. company producing these fibers, has developed a family of continuous Si-C filaments, the SCS-6 fiber family, with a coating developed to reinforce the Ti matrix. These fibers are fabricated by chemical vapor deposition (CVD) utilizing a heated carbon monofilament core spun from coal-tar pitch that acts as a nucleation site for deposition of the  $\beta$  Si-C material. Each core filament is drawn through a glass-tube reactor, where electrodes contact the fiber and heat it by electrical resistance. Silane and hydrocarbon vapors enter the reactor and decompose, depositing Si-C on the fiber as it passes through. Because of the extreme reactivity of the Ti matrix with Si-C at temperatures greater than 1,600 °F, a coating must be used on the Si-C fiber. The fiber itself is a complicated composite, consisting of many different layers of  $\beta$  Si-C deposited on the carbon core with different carbonaceous coatings covering the Si-C layers. A Si-C fiber cross-section showing the various deposition zones including the unique surface zone that provides superior tailored matrix bonding is shown in figure 35.<sup>17</sup> For the detailed structural and chemical aspects of each layer of this fiber, the reader is referred to X.J. Ning and P. Pirouz, *Journal of Materials Research*, vol. 6, No. 10, October 1991. For fiber processing details, the reader is referred to P.R. Hoffman, Textron President, "Processing of Fiber Reinforced Titanium Composites," Second ASM Paris Conference, September 1991.

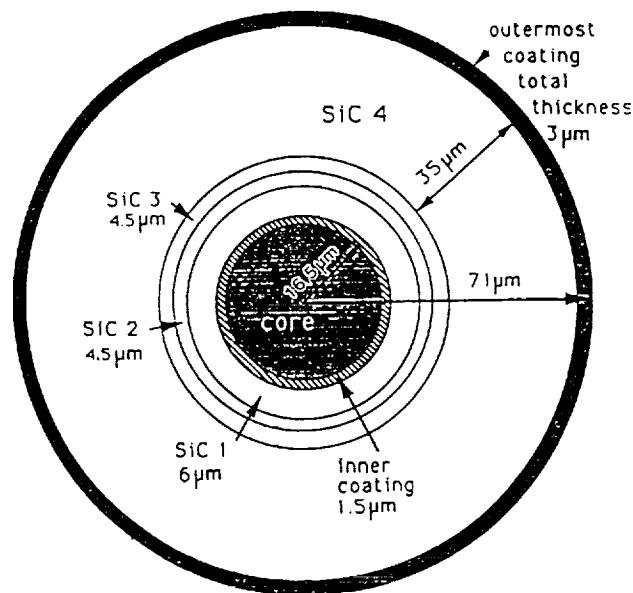


Figure 35. Si-C fiber microstructure.

The outer layer of the resulting strand is made carbon rich so that the Ti matrix cannot penetrate the fiber and reduce its strength. The  $\beta$  Si-C is present as such across all of the fiber cross-section except the last few micrometers at the surface where, by altering the gas flows in the bottom of the tubular reactor, the surface composition and structure are modified by an addition of amorphous carbon that heals the crystalline surface for improved surface strength, followed by a modification of the Si to C ratio to provide improved bonding with the metal. The surface of the Si-C fiber must be tailored to the

matrix. One type fiber has been combined with Al to form the MMC which is used for tactical missile fuselages and for carrying primary structural loads in the space shuttle orbiter. The fiber used is 35 percent 6Al-Ti-4V and 48 percent 6061 Al. Peak deposition temperature is 2,370 °F. Above this grain growth results, and below this internal property degradation stresses occur. These Si-C fibers handle the primary loads and have a tensile strength of over 550 ksi, a modulus of over 58 m/in<sup>2</sup>, and a density of 0.11 lb/in<sup>3</sup>. They are currently produced in two diameters, 5.6 and 3 mil. Figure 36 shows the tensile strength versus time at temperature of the SCS-9/ $\beta$  21S composite.<sup>17</sup>

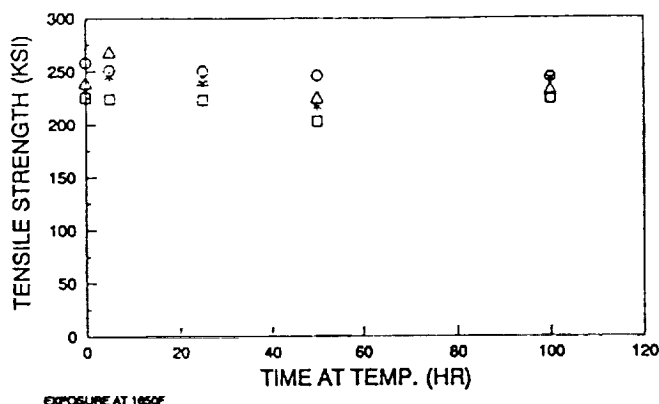


Figure 36. Tensile exposure result of SCS-9/ $\beta$  21S composite.

A number of techniques are used for composite fabrication using either foil or powder matrix material in combination with a continuous fiber. These include hot isostatic pressing, vacuum hot pressing, arc spraying, plasma spraying, powder cloth technique, electron beam vapor deposition, and a woven fiber mat. Thermal expansion and chemical compatibility between the fiber and the matrix are the major challenges to the fabrication of these high performance composites. Studies of TMC's have shown that reaction between the Ti<sub>3</sub>-Al matrix and Si-C-based fiber is less than that of Ti-6Al-4V/Si-C composites, and that with increasing Nb addition to Ti<sub>3</sub>-Al the reaction zone width decreases. Textron has developed the SCS-6/(Ti-24Al-11Nb) with excellent properties. The new  $\beta$  will have improved fiber and matrix CTE compatibility over the  $\alpha$ -2.

In the processing of a TMC, the principle objective is to firmly embed the fiber within the matrix while achieving uniform spacing of the fibers without voids or delamination and providing a tailored interfacial bond between fiber and matrix. In general, and as is done for Si-C/Al, this is done at or near molten metal temperature. However, Ti is extremely reactive at elevated temperature. To alleviate reactions at the fiber/matrix interface which reduce strength, the processing temperature is reduced. This requires a solid-state high-pressure consolidation process that demands careful control of metal placement.<sup>17</sup>

Textron uses two techniques for turning the Si-C fibers into preform sheets with Ti. In the first, Si-C fiber is wound around a large circular drum with the desired spacing. After the drum is placed in an argon-filled chamber, a hot Ti plasma is sprayed over and around the strands, bonding to them and forming the metal matrix of a monotape up to 10-ft long and 2-ft wide. The other method is weaving. Single-arm rapier looms and shuttle looms are used to produce mats of 100 to 140 reinforcing fibers per inch which are held together by a cross-weave of Ti ribbons. Next, the fiber weaves are sandwiched between layers of Ti foil about 0.005-in thick. Varying the orientation of Si-C fibers from layer to layer increases the final strength of the TMC. Fiber content of TMC preform sheets is typically 35 percent by volume (fig. 37).<sup>17</sup>

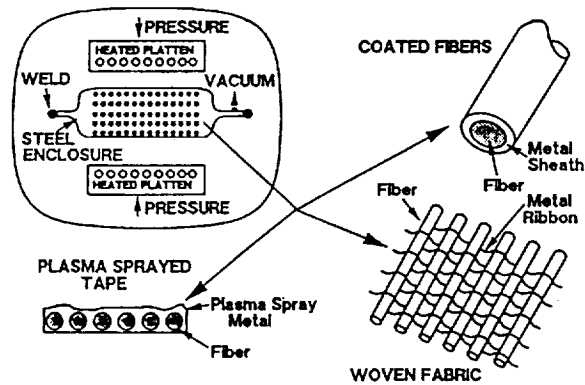


Figure 37. Fiber preforms.

The foil and fiber-weave sandwiches, or the plasma-sprayed preforms, are then laid up in clean rooms into a mold, which is then placed in a steel "bag." The bag is a rectangular, flat steel frame that contains the mold. The upper and lower skins of the 0.024-in thick sheet steel are placed over the frame and welded to it, forming the complete sealed bag. A vacuum is then imposed by evacuating the air from the steel bag. The skins are thick enough to prevent tearing as they compress at high temperature, but do not restrict movement. Next is the hot isostatic press (HIP) (fig. 38), where the material is heated.<sup>17</sup>

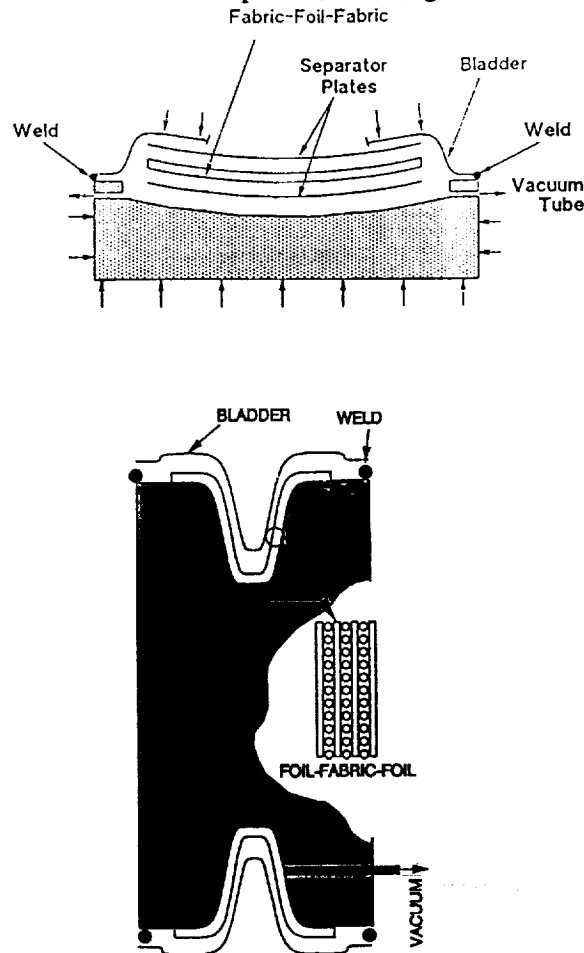


Figure 38. HIP processing of skin panels and stiffeners.

The gas pressure deforms the bladder which consolidates the composite against the mold. HIP conditions are 15 ksi pressure at temperatures up to 2,350 °F for a consolidation time of 2 to 4 hr. After the HIP process, the fixture is flame-cut open, and final trimming is done with a water-jet cutter that uses garnet in suspension. Tubular TMC parts are HIP processed between concentric cylinders. Large parts, such as L/V control surfaces, and complicated parts use a HIP, similar to an autoclave but which operates at higher temperatures and pressures. Diffusion-bonding TMC parts to one another can be done during HIP processing or in a separate operation such as an autoclave.<sup>17</sup>

TMC materials are subjected to extensive testing to provide mechanical information about the interfacial bond strength between matrix and reinforcement. Figure 39 shows the top and underside of a Ti-6Al-4V/35 percent volume Si-C monofilament composite wedge after testing.<sup>22</sup> In Textron's inspection facilities, many methods are used on TMC parts which include x ray, ultrasound, and scanning electron microscopes. Textron maintains a comprehensive network of laboratories that provide full material property assessment and ballistic evaluation.<sup>17</sup> Interfacial chemical reactions are a concern for Ti composites, because Ti and its alloys tend to react with most candidate reinforcements. The diffusion bonding process commonly used in fabricating TMC's can cause significant interfacial reaction when the reinforcement is Si-C monofilament. Table 16 shows interfacial shear strength.<sup>22</sup>

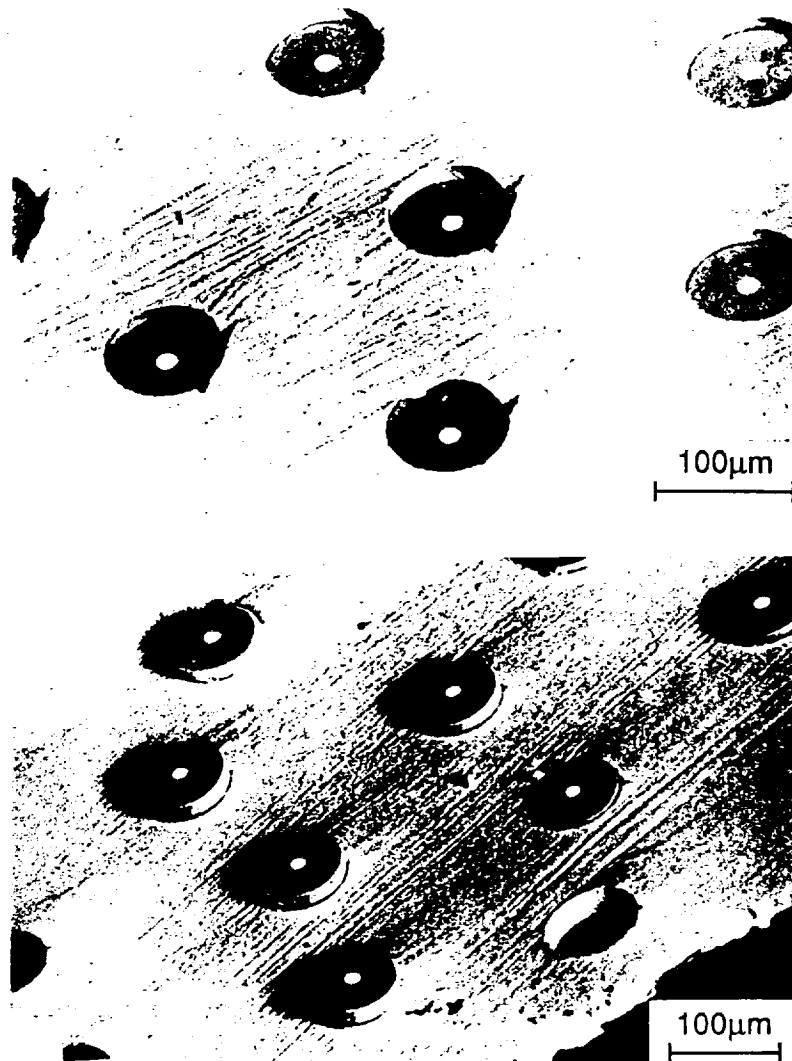
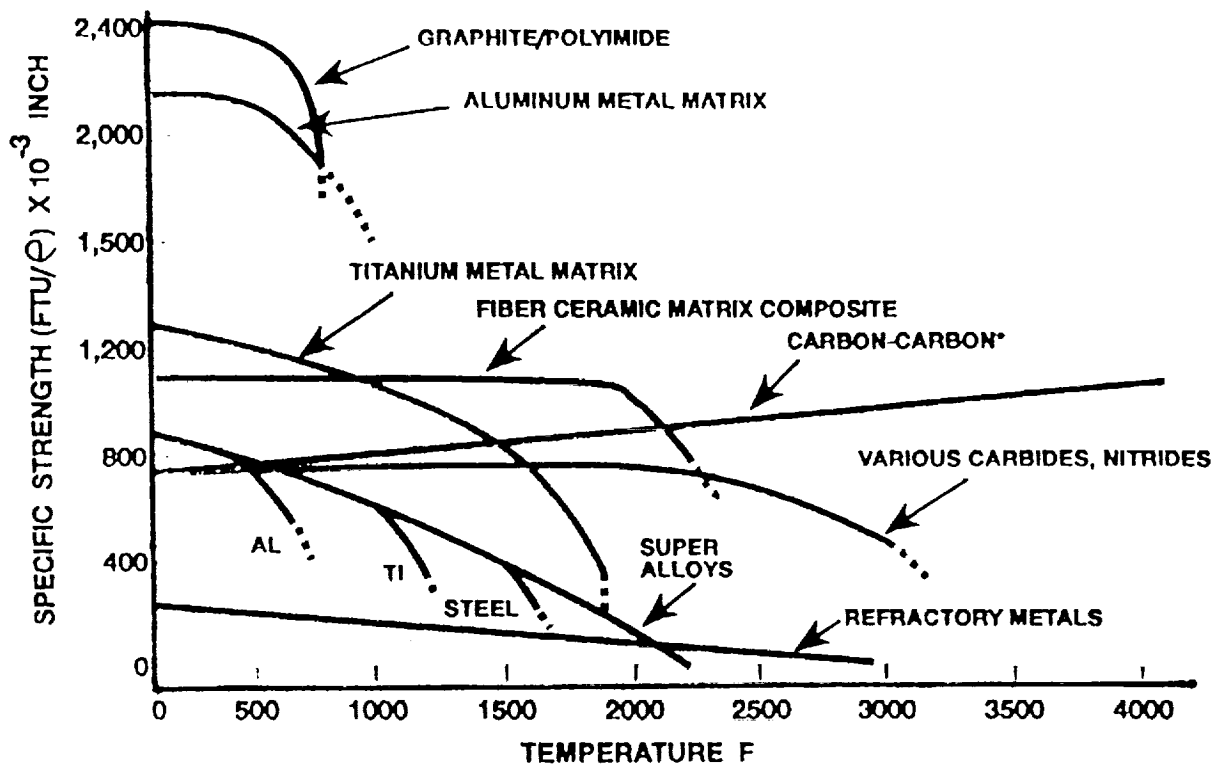


Figure 39. TMC bond strength after testing as depicted by electron micrograph.

Table 16. Interfacial shear strength of TMC.

Matrix	Si-C fiber	Processing	Test method	$\tau^*$ (MPa)	$\tau_{fr}$ (MPa)	Ref.
Ti	Sigma-1	spray deposit	pull-out	50	12	60
Ti-6Al-4V	Sigma-1	diffusion bond	fragmentation	345	—	35
Ti-6Al-4V	Sigma-2	diffusion bond	push-out	—	80	52
Ti-6Al-4V	Sigma-2	diffusion bond, 59 h at 815 °C	push-out	—	211	52
Ti-25Al-10Nb-3V	SCS-6	powder hot press	push-out	110	57	44
Ti-25Al-10Nb-3V	SCS-6	powder hot press, 100 h at 800 °C	push-out	99	59	44
Ti-6Al-4V	SCS-6	diffusion bond	push-out	150	90	44
Ti-15V-3Al-3Cr-3Sn	SCS-6	diffusion bond	push-out	120	80	44
Ti-25Al-10Nb-3V	SCS-6	diffusion bond	push-out	120	50	44
Ti	SCS-6	spray deposit	pull-out	5	1	60
Ti-6Al-4V	SCS-6	diffusion bond	fragmentation	180	—	35
Ti-6Al-4V	B or Si-C	diffusion bond	fragmentation	240	—	35

Figure 40 compares the high-temperature strengths of many of the advanced materials<sup>17</sup> discussed in this paper, and table 17 compares tensile properties of TMC's and other MMC's.<sup>3</sup> Additionally, use of TMC material requires less thermal protection which is a considerable cost savings.



\* COATING STATE-OF-THE-ART TEMPERATURE LIMIT

Figure 40. Strength comparisons of advanced materials.

Table 17. Tensile properties of TMC's and other MMC's.

Material	Tensile strength, MPa (ksi)	Tensile modulus, GPa (Msi)
6061-T6 aluminum alloy	306 (44.4)	70 (10)
T-300 carbon-6061 Al alloy ( $v_f = 35$ to 40 percent)	1,034 to 1,276 (L) (150 to 185)	110 to 138 (L) (15.9 to 20)
Boron-6061 Al alloy ( $v_f = 60$ percent)	1,490 (L) (216) 138 (T) (20)	214 (L) (31) 138 (T) (20)
Particulate Si-C-6061-T6 Al alloy ( $v_f = 20$ percent)	552 (80)	119.3 (17)
GY-70 carbon-201 Al alloy ( $v_f = 37.5$ percent)	793 (L) (115)	207 (L) (30)
Al <sub>2</sub> -O <sub>3</sub> -Al alloy ( $v_f = 60$ percent)	690 (L) (100) 172 to 207 (T) (25 to 30)	262 (L) (38) 152 (T) (22)
Ti-6Al-4V titanium alloy	890 (129)	120 (17.4)
Si-C-Ti alloy ( $v_f = 35$ to 40 percent)	820 (L) (119) 380 (T) (55)	225 (L) (32.6) —
SCS-6-Ti alloy ( $v_f = 35$ to 40 percent)	1,455 (L) (211) 340 (T) (49)	240 (L) (34.8)

## XVI. CONCLUSIONS

Due to the aft cg locations on many L/V's currently being studied, the need has arisen for the vehicle control augmentation that is provided by aerodynamic flight controls. In the Saturn era, NASA went to the Moon with 300 ft<sup>2</sup> of aerodynamic surfaces on the Saturn V. Since those days, a plethora of advanced composites and smart materials has been developed that enables the design of very lightweight, strong, and innovative L/V aerodynamic flight control surfaces.

The new MMC's can not only provide substantial weight savings and increased high-temperature strength, which allow increased payload capability and flight performance, but can also reduce the thermal protection requirements, thus providing even more indirect weight and cost savings. TMC's have already been selected by NASA for the NASP, and appear to be among the candidates in the advanced composites for use on L/V flight control surfaces.

Many of the smart materials can be used as both sensors and actuators, and by physically deforming themselves can produce significant actuation forces. Patents have recently been granted on

articulated flight control surfaces using SMA's. The replacement of conventional flight control actuation systems could result in enormous savings in cost and weight. Smart materials with embedded sensors and actuators could damp undesirable vibration modes as a L/V goes through the subsonic, transonic, and supersonic speed regimes in the ascent trajectory.

As more L/V's are designed with aft cg's, and as hypersonic flight research proceeds, smart materials and advanced composites can lend themselves to very attractive aerodynamic flight control solutions to flight stability and control challenges. This brief overview has hopefully winnowed out from the burgeoning array of literature and provided insight to those which are directly applicable to flight control surfaces of a L/V. Nowhere in the literature has there been found any application of smart materials or advanced composites to the flight controls of an expendable, large Saturn class L/V.



## REFERENCES

1. Culshaw, B., et al. (ed.): "First European Conference on Smart Structures and Materials," Conference Proceedings, Glasgow, May 1992
2. Jardine, P.A., et al. (ed.): "Smart Materials Fabrication and Materials for Micro-Electro-Mechanical Systems," Symposium Proceedings, Materials Research Society, 1992.
3. Wada, B.K., et al. (ed.): "Third International Conference on Adaptive Structures," Conference Proceedings, San Diego, CA, November 1992.
4. Gandhi, M.V., and Thompson, B.S.: "Smart Materials and Structures." Chapman and Hall, 1992.
5. Newnham, R.E., and Ruschan, G.R.: "Smart Electroceramics." American Ceramic Society Journal, March 1991.
6. NASA Technical Briefs, October 1993.
7. NASA Langley Research Center: "A State-of-the-Art Assessment of Active Structures." NASA TM 107681, September 1992.
8. Coulter, J.P., and Weiss, K.: "Engineering Applications of Electrorheological Materials." Journal of Intelligent Material Systems and Structures, vol. 4, No. 2, April 1993.
9. Moran-Lopez, J.L., and Sanches, J.M. (ed.): "Advanced Topics in Materials Science and Engineering," Conference Proceedings, Mexico, September 1991, Plenum Press, 1991.
10. Cincotta, M., et al.: "Articulated Control Surface." U.S. Patent No. 5,114,104, May 19, 1992.
11. Beauchamp, C.H., et al.: "Articulated Fin/Wing Control System." U.S. Patent No. 5,186,420, February 16, 1993.
12. Aerospace America, October 1992.
13. Mallick, P.K.: "Fiber-Reinforced Composites." Marcel Dekker, Inc., 1993.
14. "Advanced Composite Materials," Conference Proceedings, Detroit, MI, ASM International, October 1991.
15. Weeton, J.W., et al.: "Engineer's Guide to Composite Materials." American Society for Metals, 1987.
16. Han, Yafang, (ed.): "Advanced Structural Materials," Symposia Proceedings, Beijing, China, June 1990, Elsevier, 1991.
17. Visit to Textron Specialty Materials Company in Lowell, Massachusetts; Plant Tours and Launch Vehicle Flight Control Surface Design Review held with: Melvin Mitnick, Director of Product Applications; Dr. Al Kumnick, Director of Research and Development; Bill Grant, Director of

Fabrication; Monte Treasure, Director of Operations; John Hackem, TMC Plant Manager; and input from publications by Textron President, Dr. Paul R. Hoffman; September 29–30, 1993.

18. Buckley, J.D., (ed.): "Carbon-Carbon Materials and Composites." Noyes Publications, 1993.
19. Vincenzini, (ed.): "Advanced Structural Inorganic Composites," Symposium Proceedings, Italy, June, 1990, Elsevier, 1991.
20. Lemkey, F.D., et al. (ed.): "High Temperature/High Performance Composites," Symposium Proceedings, Materials Research Society, 1988.
21. Taha, M.H., and El-Mahallawy, N.A., (ed.): "Advances in Metal Matrix Composites Conference," Conference Proceedings, Cairo, Egypt, 1993.
22. Clyne, T.W., and Withers, P.J.: "An Introduction to Metal Matrix Composites." Cambridge University Press, 1993.

REPORT DOCUMENTATION PAGE			Form Approved OMB No. 0704-0188	
Public reporting burden for this collection of information is estimated to average 1 hour per response, including the time for reviewing instructions, searching existing data sources, gathering and maintaining the data needed, and completing and reviewing the collection of information. Send comments regarding this burden estimate or any other aspect of this collection of information, including suggestions for reducing this burden, to Washington Headquarters Services, Directorate for Information Operations and Reports, 1215 Jefferson Davis Highway, Suite 1204, Arlington, VA 22202-4302, and to the Office of Management and Budget, Paperwork Reduction Project (0704-0188), Washington, DC 20503.				
1. AGENCY USE ONLY (Leave blank)	2. REPORT DATE February 1995	3. REPORT TYPE AND DATES COVERED Technical Paper		
4. TITLE AND SUBTITLE Launch Vehicle Flight Control Augmentation Using Smart Materials and Advanced Composites (CDDF 93-05)		5. FUNDING NUMBERS		
6. AUTHOR(S) C. Barret				
7. PERFORMING ORGANIZATION NAME(S) AND ADDRESS(ES) George C. Marshall Space Flight Center Marshall Space Flight Center, Alabama 35812		8. PERFORMING ORGANIZATION REPORT NUMBER  M-770		
9. SPONSORING/MONITORING AGENCY NAME(S) AND ADDRESS(ES) National Aeronautics and Space Administration Washington, DC 20546		10. SPONSORING/MONITORING AGENCY REPORT NUMBER  NASA TP-3535		
11. SUPPLEMENTARY NOTES  Prepared by Structures and Dynamics Laboratory, Science and Engineering Directorate.				
12a. DISTRIBUTION/AVAILABILITY STATEMENT  Subject Category: 15 Unclassified-Unlimited		12b. DISTRIBUTION CODE		
13. ABSTRACT (Maximum 200 words)  The Marshall Space Flight Center has a rich heritage of launch vehicles that have used aerodynamic surfaces for flight stability such as the Saturn vehicles and flight control such as on the Redstone. Recently, due to aft center-of-gravity locations on launch vehicles currently being studied, the need has arisen for the vehicle control augmentation that is provided by these flight controls. Aerodynamic flight control can also reduce engine gimballing requirements, provide actuator failure protection, enhance crew safety, and increase vehicle reliability, and payload capability. In the Saturn era, NASA went to the Moon with 300 ft <sup>2</sup> of aerodynamic surfaces on the Saturn V.  Since those days, the wealth of smart materials and advanced composites that have been developed allow for the design of very lightweight, strong, and innovative launch vehicle flight control surfaces. This paper presents an overview of the advanced composites and smart materials that are directly applicable to launch vehicle control surfaces.				
14. SUBJECT TERMS smart flight controls, flight control surfaces, launch vehicle control, advanced composites, smart materials, sensors, shape memory alloys, metal matrix composites, titanium matrix composites			15. NUMBER OF PAGES 55	
			16. PRICE CODE A04	
17. SECURITY CLASSIFICATION OF REPORT Unclassified	18. SECURITY CLASSIFICATION OF THIS PAGE Unclassified	19. SECURITY CLASSIFICATION OF ABSTRACT Unclassified	20. LIMITATION OF ABSTRACT Unlimited	





National Aeronautics and  
Space Administration  
Code JTT  
Washington, DC  
20546-0001

*Official Business*  
*Penalty for Private Use, \$300*

*Postmaster: If Undeliverable (Section 158 Postal Manual), Do Not Return*

---